



<https://theses.gla.ac.uk/>

Theses Digitisation:

<https://www.gla.ac.uk/myglasgow/research/enlighten/theses/digitisation/>

This is a digitised version of the original print thesis.

Copyright and moral rights for this work are retained by the author

A copy can be downloaded for personal non-commercial research or study,
without prior permission or charge

This work cannot be reproduced or quoted extensively from without first
obtaining permission in writing from the author

The content must not be changed in any way or sold commercially in any
format or medium without the formal permission of the author

When referring to this work, full bibliographic details including the author,
title, awarding institution and date of the thesis must be given

Enlighten: Theses

<https://theses.gla.ac.uk/>
research-enlighten@glasgow.ac.uk

THE NUCLEAR SCATTERING OF HIGH ENERGY PHOTONS

BY

HENRY S. CAPLAN

Submitted to the University of Glasgow as a Thesis
for the degree of Doctor of Philosophy.

October, 1959.

ProQuest Number: 10656272

All rights reserved

INFORMATION TO ALL USERS

The quality of this reproduction is dependent upon the quality of the copy submitted.

In the unlikely event that the author did not send a complete manuscript and there are missing pages, these will be noted. Also, if material had to be removed, a note will indicate the deletion.



ProQuest 10656272

Published by ProQuest LLC (2017). Copyright of the Dissertation is held by the Author.

All rights reserved.

This work is protected against unauthorized copying under Title 17, United States Code
Microform Edition © ProQuest LLC.

ProQuest LLC.
789 East Eisenhower Parkway
P.O. Box 1346
Ann Arbor, MI 48106 – 1346

PREFACE

This thesis describes an investigation by the author of the scattering of high energy photons by carbon nuclei.

When he started his research in October, 1956 the decision to attempt the experiment had been made but no instrumentation for it had been constructed. The author then constructed nearly all the necessary electronics and helped in the construction of a total absorption gamma-ray Cerenkov spectrometer built round a single crystal of lead fluoride kindly made available to this laboratory by Professor R. V. Jones of Aberdeen University.

This counter, after testing, proved to have insufficient energy resolution for the photon scattering experiment but the experience gained from it was applied by the author to the building of the similar but much larger instrument using lead glass instead of lead fluoride described in Chapter 11, Section 11.

The work of designing the experiment, the construction of the scintillation counter telescope (Chapter 11, Section 111), and the collection of data during the runs on the departmental electron synchrotron was shared with Dr. W. S. C. Williams and later also with Dr. D. T. Stewart who had joined the group. The author however, was solely responsible for the analysis of the results given in Chapter 14.

The author is greatly indebted to Dr. W. S. C. Williams for his close guidance and would like to acknowledge the help given by Dr. D. T. Stewart with his fresh outlook on the experiment.

Thanks are also due to the synchrotron crew under Dr. W. McFarlane for their help and patience, particularly during the low intensity runs.

The author would also like to thank Professor P. I. Dee for his warm interest and encouragement in the above researches.

The contribution made to the project by the workshop staff and the departmental technicians deserves recognition.

Finally, the author is indebted to the Department of Scientific and Industrial Research for the maintenance grant which enabled him to carry out the three years of research.

Henry S. Goplan.

CONTENTS

	page
Preface	-
 CHAPTER I.	
Section I. General Background	1
Section II. Review of Previous Theoretical Work	
1. The Scattering of Photons by Nucleons	3
2. The Scattering of Photons by Complex Nuclei	10
Section III. Review of Previous Experimental Work	
1. The Scattering of Photons by Protons	19
2. The Scattering of Photons by Complex Nuclei.	26
 CHAPTER II. THE INSTRUMENTATION OF THE PHOTON SCATTERING EXPERIMENT.	
Section I. The Experimental Requirements	33
Section II. The Cerenkov Total Absorption Spectrometer	
1. The Construction of the Spectrometer	35
2. The Testing of the Spectrometer	39
3. The Calibration of the Spectrometer	41
Section III. The Scintillation Counter Telescope	
1. The Purpose and Principle of Operation	45
2. The Construction and Testing	46
Section IV. The Electronic Circuitry	50
 CHAPTER III. THE PHOTON SCATTERING EXPERIMENT	
Section I. General Considerations	53
Section II. Experimental Procedure	55

(contd)

CONTENTS

	page
Section 111. The Absolute Cross-Section	59
CHAPTER IV. ANALYSIS AND RESULTS	62
CHAPTER V. DISCUSSION AND CONCLUSIONS	70

List of Figures

	Opposite page
1. The Predictions of Powell and Klein and Nishina	5
2. The Predictions of Field Theories	6
3. The Predictions of Semi-phenomenological Theories	7
4. The Predictions of Dispersion Theories	8
5. The Origin of the Maximum in the Differential Cross-section in the Backward Direction	9
6. The Form Factor f^2 Evaluated for Scattering from the Carbon nucleus	16
7. The Predicted Cross-section at 90°	17
8. The Predicted Angular Distribution	17
9. The Results of Oxley and Telegdi Compared with the Predictions of Powell, Klein and Nishina and Goldberger et al.	21
10. The Comparison of the Experimental Results with the best Theoretical Predictions	24
11. Diagrammatic View of the Cerenkov Spectrometer	37
12. View of the Cerenkov Spectrometer Showing the Magnetic Screening	38
13. View of the Cerenkov Spectrometer Showing the Construction	38
14. The Calibration of the Cerenkov Spectrometer	41
15. The Response of the Cerenkov Spectrometer to 100 Mev. Electrons	42
16. Variation of Mean Pulse Height with Energy	43
17. Variation of Resolution with Energy	43

(contd)

List of Figures

Opposite
page

18.	A Photon Sensitive Scintillation Counter Telescope	45
19.	The Construction of the Scintillation Counters	45
20.	The Coincidence Telescope, Magnetic Screen and Cooling Fan	46
21.	Curve Indicating the Equality of Transit Time of Two Phototubes	48
22.	Block Diagram of Electronics	50
23.	The Layout of the Cerenkov Spectrometer and the Counter Telescope for the Photon Scattering Experiment	54
24.	The Response of the Detection System to the Bremsstrahlen	68
25.	The Variation of Cross-section with Energy. (1) 90° , (2) 112° and (3) 135°	69
26.	The Experimental Angular Distribution	69
27.	The Semi-empirically Efficiency and the Experimental Mean Value	68

CHAPTER 1.SECTION 1.General Background

Perhaps most of our information about the physical world has been gained by observing the scattering of radiation. Visible light scattered into our eyes by objects tells us directly their size, shape, colour and how they are moving. To resolve the molecules and atoms of which these objects are composed, radiation whose de Broglie wavelength, λ , is at most the same order of magnitude as the linear dimensions involved ($\sim 10^{-8}$ cm.) must be used.

Some examples are given in the following table:

Radiation	Typical Energy	λ , 10^{-8} cm.
Electromagnetic	10 Kev.	0.2
Electron	10 ev.	0.6
Thermal Neutron	1/40 ev.	0.3

To gain information about the atomic nucleus and the nucleons of which it is composed is logically the next step in the sequence. In this case the distances involved are of the order of 10^{-13} cm. and the basic possibilities are summarized as before.

Radiation	Typical Energy	λ , 10^{-13} cm.
Electromagnetic	200 Mev.	1.0
Electron	200 "	1.0
Meson	50 "	1.7
Nucleon	10 "	1.4

This thesis discusses the information which can be gained from the first example in the table: The nuclear scattering of high energy photons.

SECTION 11.Review of Previous Theoretical Work.1. The Scattering of Photons by Nucleons.

The most fundamental case of nuclear scattering of photons is the scattering by individual nucleons, i.e., the reactions



Since only the first of these two reactions can be directly investigated experimentally, it will be dealt with in detail while the second will be more briefly treated.

In Analogy with the Compton Effect,



the reaction (1) is usually called the Proton Compton Effect.

The cross-section for reaction (3) is given with great accuracy by the Klein and Nishina formula. The low energy limit of this formula is the classical Thomson scattering cross-section.

$$\begin{aligned} \sigma_0^e &= \frac{8\pi}{3} \left(\frac{e^2}{mc^2} \right)^2 \\ &= 0.665 \times 10^{-24} \text{ cm}^2 \end{aligned}$$

If the proton were, like the electron, a Dirac particle the reaction (1) would also follow the Klein and Nishina formula

except for a factor involving the ratio of the rest masses of the proton and electron. In fact it is known that the proton cannot be properly described by the Dirac equation; its magnetic moment and the presence of its meson field being salient anomalies.

It has been shown however, (1), (2), (3), that at very low energy these features will not play an important role in the scattering of photons and in the limit for zero frequency light the cross-section is exactly given by the corresponding classical Thomson value..

Thus for a proton,

$$\begin{aligned}\sigma_0^P &= \frac{8\pi}{3} \left(\frac{e^2}{M_P c^2} \right)^2 \\ &= 2 \times 10^{-31} \text{ cm.}^2\end{aligned}$$

It should be noted that

$$\begin{aligned}\frac{\sigma_0^e}{\sigma_0^P} &= \left(\frac{M_P}{m} \right)^2 \\ &= 3.37 \times 10^6.\end{aligned}$$

Hence the scattering of a photon by a proton is several million times less probable than the scattering by an electron. The low energy limit of the scattering of photons by neutrons (reaction (2)) which have of course no nett electric charge is, (1), (2), (3). by the same arguments, zero.

except for a factor involving the ratio of the rest masses of the proton and electron. In fact it is known that the proton cannot be properly described by the Dirac equation; its magnetic moment and the presence of its meson field being salient anomalies.

It has been shown however, (1), (2), (3), that at very low energy these features will not play an important role in the scattering of photons and in the limit for zero frequency light the cross-section is exactly given by the corresponding classical Thomson value..

Thus for a proton,

$$\begin{aligned}\sigma_0^P &= \frac{8\pi}{3} \left(\frac{e^2}{M_P c^2} \right)^2 \\ &= 2 \times 10^{-31} \text{ cm}^2.\end{aligned}$$

It should be noted that

$$\begin{aligned}\frac{\sigma_0^e}{\sigma_0^P} &= \left(\frac{M_P}{m} \right)^2 \\ &= 3.37 \times 10^6.\end{aligned}$$

Hence the scattering of a photon by a proton is several million times less probable than the scattering by an electron. The low energy limit of the scattering of photons by neutrons (reaction (2)) which have of course no nett electric charge is, (1), (2), (3). by the same arguments, zero.

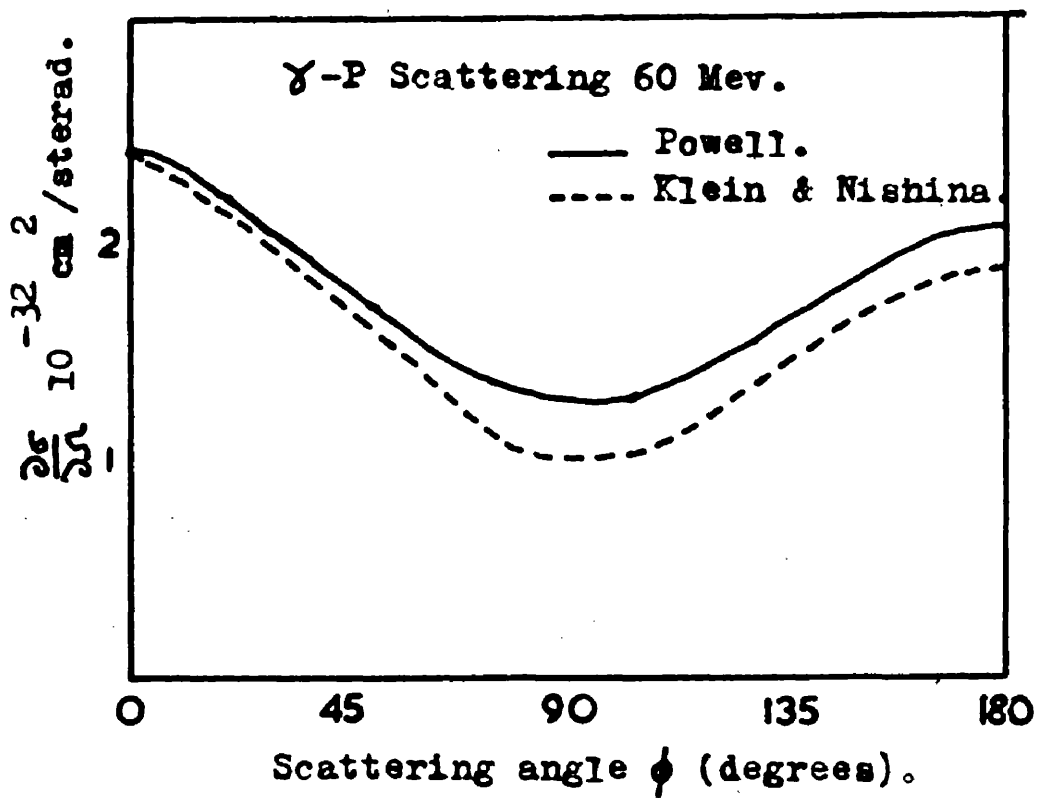


Fig. 1.

The Predictions of Powell and Klein & Nishina.

At slightly higher incident photon energies the anomalous magnetic moment will cause the scattering by protons to deviate from the Klein and Nishina formula. The simplest method of treating this is merely to add the anomalous part of the magnetic moment to the ordinary Dirac Hamiltonian as suggested by Pauli(4). The calculation of the cross-section using this modified Hamiltonian was carried out by Powell (5) in 1949. His predictions are compared with the Klein and Nishina formula in Figure (1), the two differ by about twenty-five per cent for incident photons of 100 Mev.

A more conventional approach to the anomalous magnetic moments of the nucleons is to regard them as due to currents in the cloud of virtual mesons about the nucleon core. This cloud is not rigidly connected to the core and is therefore electrically and magnetically polarisable. Such a system would be expected to contribute to the scattering of electromagnetic radiation. It was Sachs and Foldy (6)(1950) who first tackled the problem in this way. They calculated the scattering assuming a point "core" and a weakly coupled meson field. Unfortunately it was shown later that there was an error in their calculation and therefore their predictions are not given here.

In 1955 Capps and Holladay (7) calculated the cross-section replacing the point source in the pion nucleon interaction

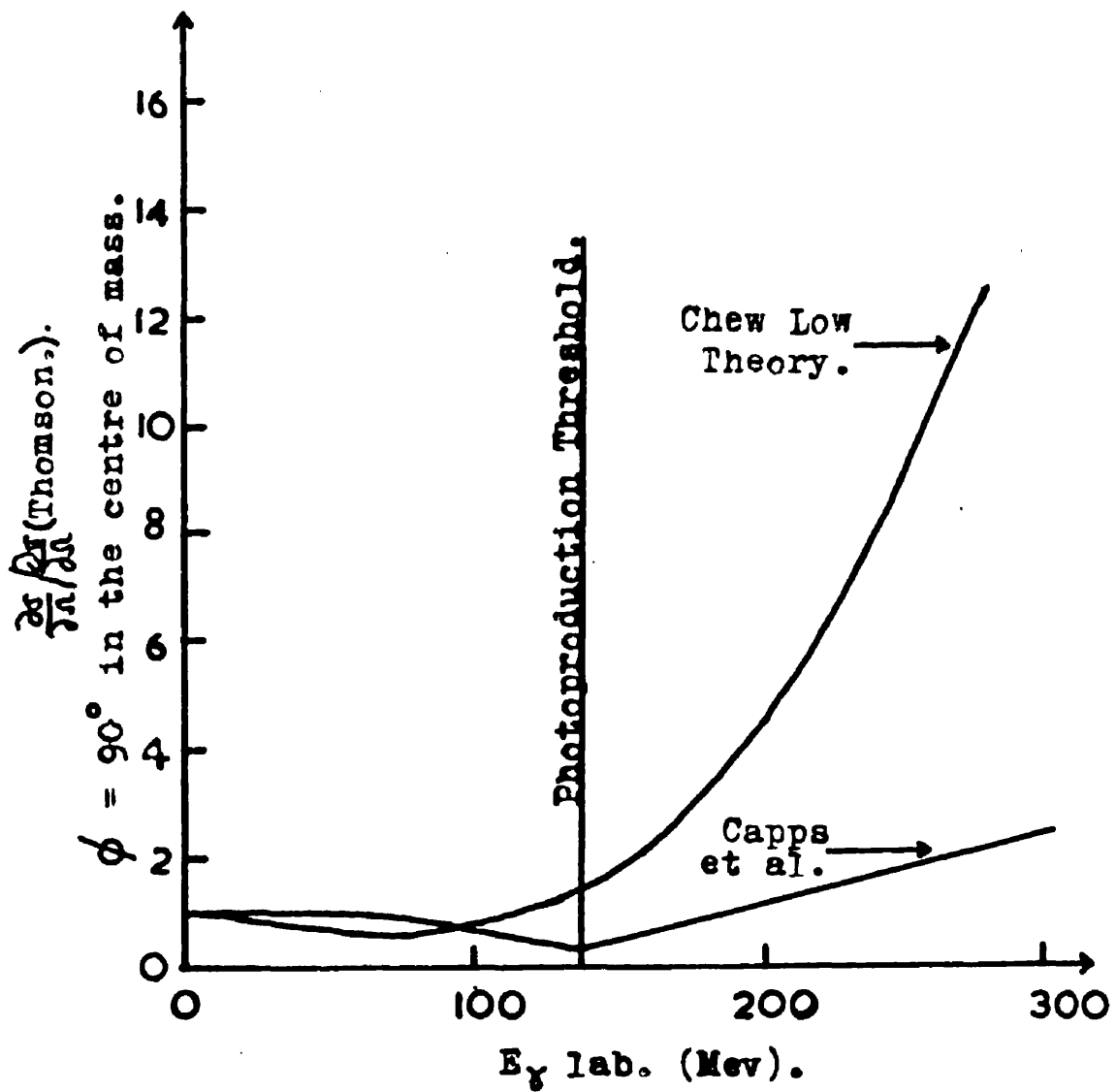


Fig. 2.

The Predictions of Field Theories.

employed by Sachs and Foldy by an extended source but retained the weak coupling approximation, Figure (2). The differential cross-sections they calculate are rather sensitive to the choice of coupling constant and are also very energy dependent. The general feature is however a forward maximum at higher photon energies. i.e. $E_{\gamma} \sim 250 \text{ Mev.}$

Very recently Karzas, Watson and Zachariasen (8) have carried out calculations for the scattering of light by protons in the framework of Chew Low formalism. Their results are compared with those of Capps et al. in Figure (2).

A semi-phenomenological analysis of the scattering of photons by nucleons which takes account of the isobaric state $I = J = \frac{3}{2}$ of the nucleon deduced from meson scattering and photoproduction data has been carried out by Austern (9), Minami (10) in Japan, and extended by Ritus (11) and independently by Gurzhi (12) in Russia. Similarly Feld (13) has obtained cross-sections for the Proton Compton Effect on his "atomic" model.

It has been reported (14) that Yamaguchi (unpublished) has further refined these calculations to include interference between spin-flip and non spin-flip terms in the scattering amplitude.

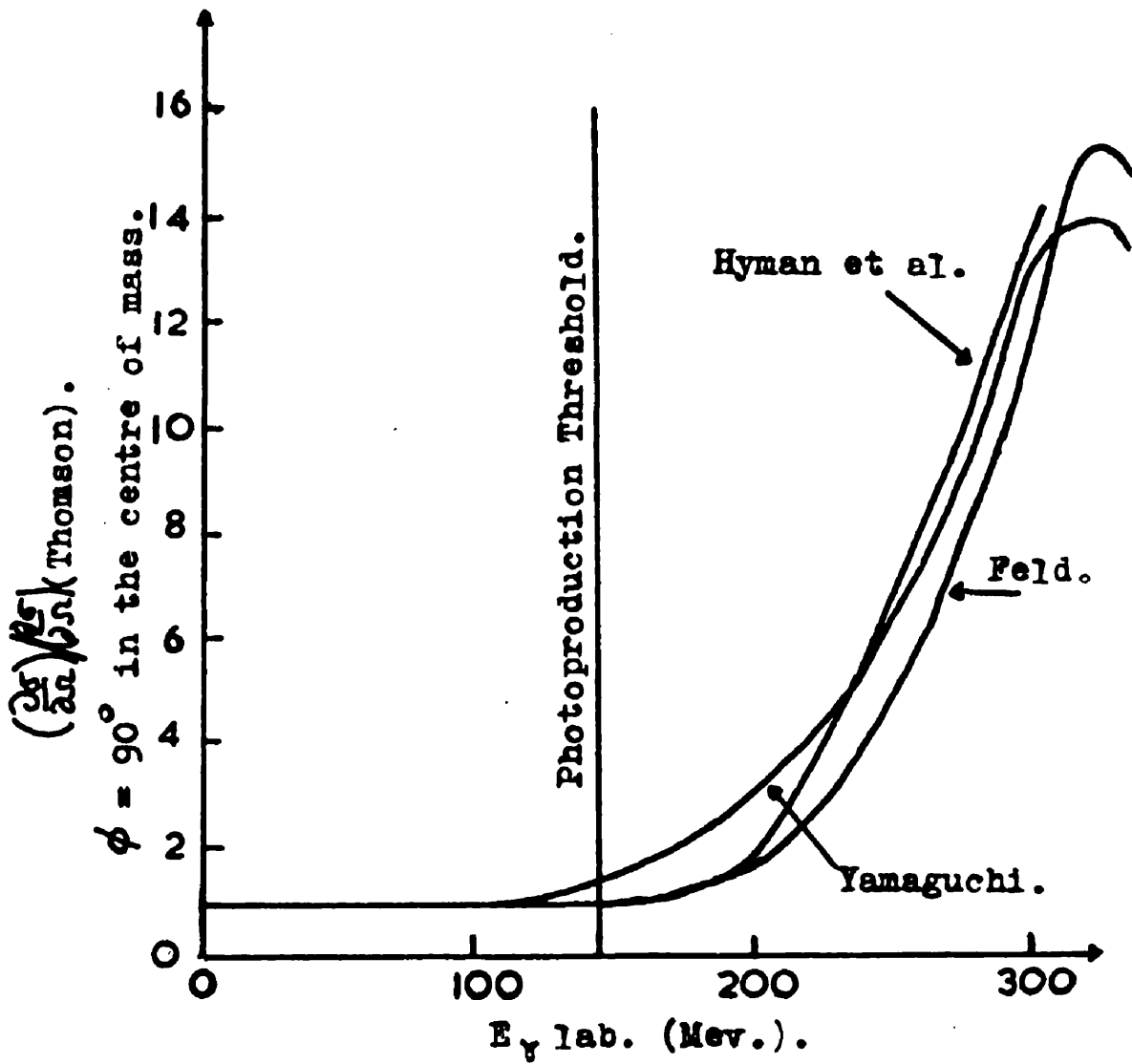


Fig. 3.

The Predictions of Semi-phenomenological Theories.

Very recently Hyman et al. (15) have also added the effect of the second excited state of the proton $I = \frac{1}{2}$, $J = \frac{3}{2}$ and some effects due to the decay of virtual π^0 mesons. The results of some of these semi-phenomenological theories are given in Figure (3).

Another theoretical approach to the problem of the scattering of electromagnetic radiation by nucleons is through the dispersion relations.

The initial work was done by Goldberger, Gell-Mann and Thirring (16) who derived dispersion relations for the spin independent and spin dependent photon-nucleon amplitudes and showed that the spin independent forward amplitude (coherent amplitude) may be determined from a knowledge of the behaviour as a function of energy of the total cross-section for the production of mesons by an unpolarised beam of photons.

The extension of the theory to angles other than 0° involves the use of some kind of model. This was done by Capps (17) who assumed that only dipole ~~photons~~^{radiation} scatters and also used some meson photoproduction and scattering data. He predicts a backward maximum in the differential cross-section in contradiction of his own work with Holladay (7) already mentioned.

Cini and Stroffolini (18) have approached the problem

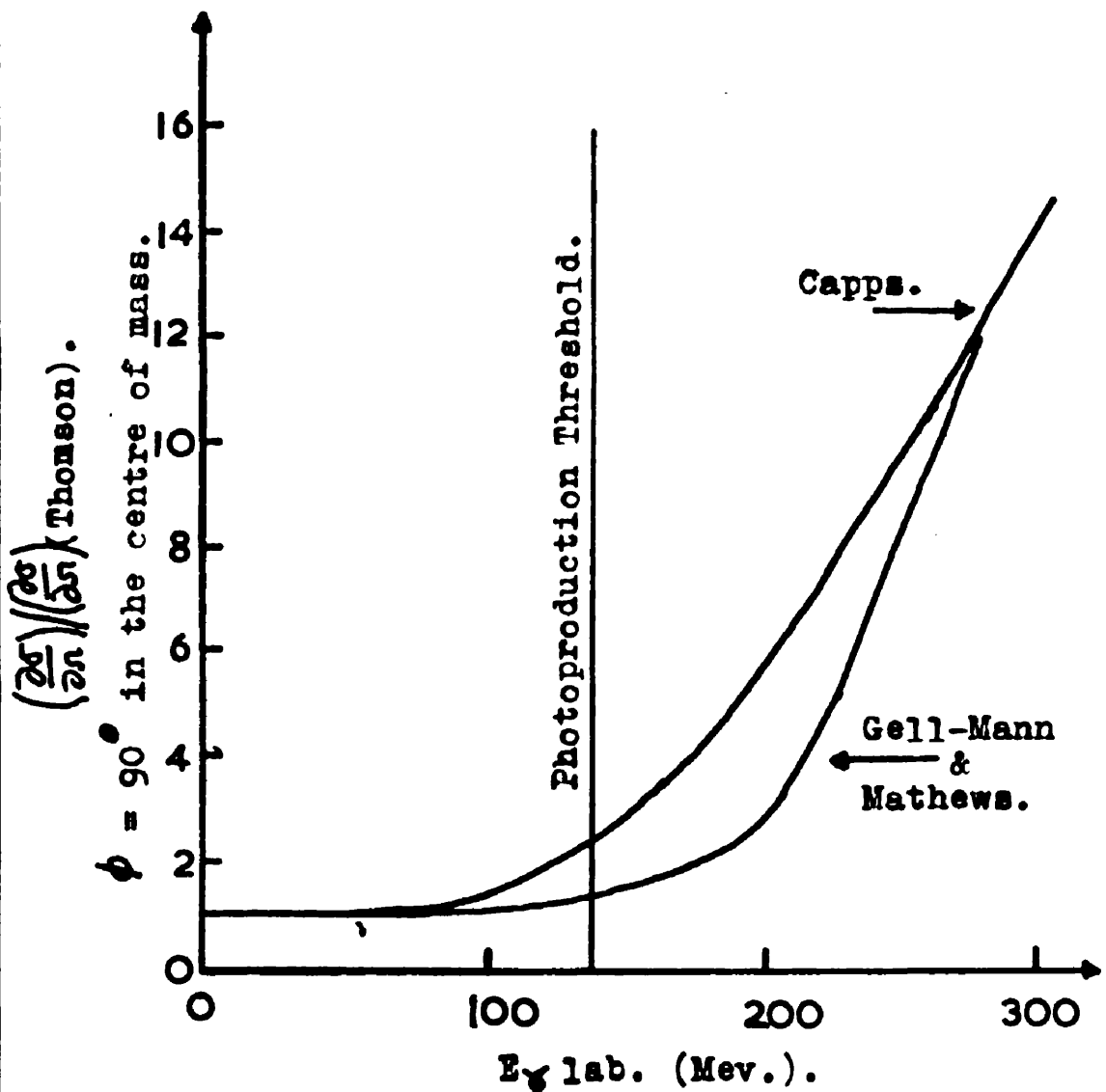


Fig. 4.

The Predictions of Dispersion Theories.

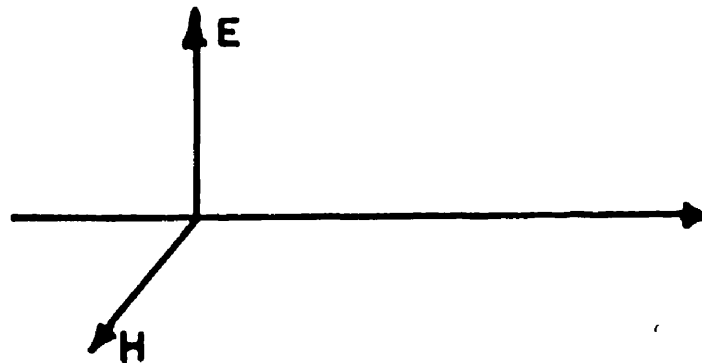
with a different attitude of mind. Their paper discusses how an experimental determination of γ -P scattering could be used as a test of the validity of the dispersion relations. They show that measurement of the differential cross-section from 45° upwards would be a significant test and only deduce the scattering cross-sections as a by-product.

The most recent and thorough investigation using these relations is that of Gell-Mann and Mathews (19) (unpublished). This work is rather esoteric but the general features are as follows. They formulated dispersion relations without the difficulties of subtraction of infinite quantities often met in this work. Having derived the forward scattering amplitude from the Optical Theorem, they calculated the differential cross-sections using the meson photoproduction data in a manner similar to that of Capps (17). Their results are shown in Figure (4).

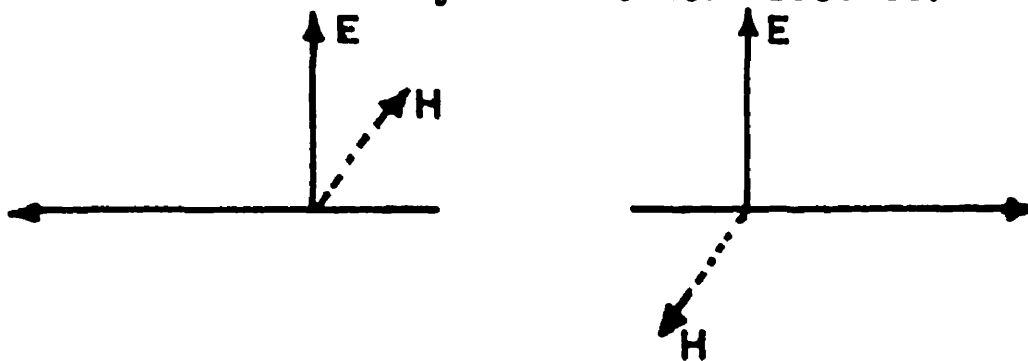
In view of the host of theoretical curves, the author feels obliged to point out the general features these have in common. In the low energy region up to meson photoproduction threshold the theoretical curves almost follow the Klein and Nishina formula. In the region above the threshold they closely approximate to a one level resonance formula.

The majority of the angular distributions predicted

Radiation Incident.



Radiation Scattered by the Thomson Process.



Radiation Scattered by the Magnetic Dipole Resonance

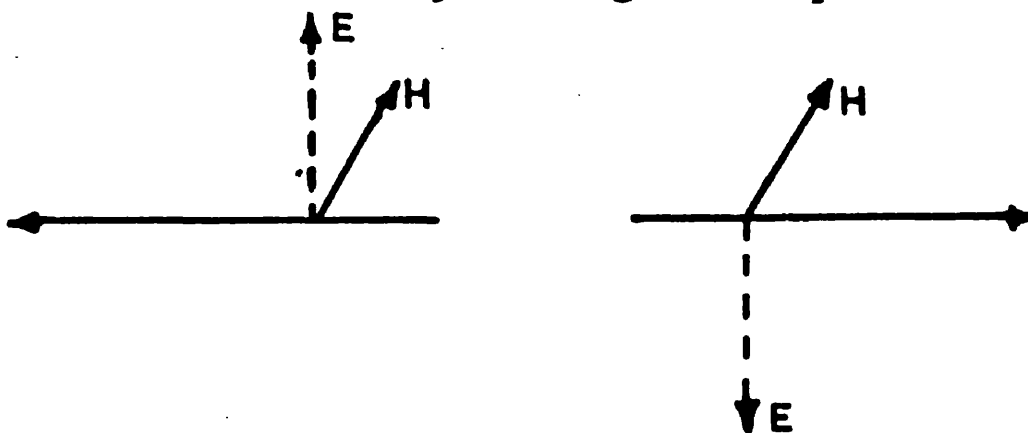


Fig. 5.

The Origin of the Maximum in the Differential Cross-section in the Backward Direction.

follow the Klein and Nishina shape in the low energy region but show a backwards maximum as the total cross-section climbs the slope of the resonance. To predict this behaviour qualitatively is very simple and does not require complicated theoretical arguments.

The maximum in the backward direction arises in the following way. There are two main factors contributing to the scattering. The first is the Thomson scattering amplitude. Classically this corresponds to the bulk motion of the proton under the influence of the electric vector of the incident radiation. In this case the electric vector of the scattered radiation is in phase with the electric vector of the incident radiation Figure (5). The other factor is the scattering due to the low energy tail of the magnetic dipole resonance. Since the frequency of the incident radiation is far below the frequency of the resonance, the magnetic vector of the scattered radiation is 180° out of phase with the magnetic vector of the incident radiation. As shown in Figure (5) this leads to destructive interference in the forward direction; on the other hand the back-scattered wave is enhanced and therefore the cross-section has a backward maximum.

The comparison with experiment of the best theoretical work discussed in this section is carried out in Section III, of this chapter.

2. The Scattering of Photons by Complex Nuclei.

Having dealt with the main features of the scattering by individual nucleons, the next step is the extension of the theory to complex nuclei.

Considering first the low energy limit as before, from the same very general arguments the cross-section will have the classical Thomson value. Thus for a nucleus of charge Z and mass A we have;

$$\begin{aligned}\sigma_0^{Z,A} &= \frac{8\pi}{3} \left(\frac{Z^2 e^2}{A M c^2} \right)^2 \\ &\doteq \sigma_0^P \frac{Z^4}{A^2}\end{aligned}$$

Since $A \doteq 2Z$ this implies an approximately Z^2 variation of the cross-section.

When slightly higher photon energies are considered the situation becomes very complicated due to the nuclear energy levels and the competition of photodisintegration reactions.

To separate these two effects, the energy region below particle emission threshold is considered first. Here the cross-section will be dominated by resonance scattering. The maximum cross-section (σ_{max}) for the absorption of a dipole photon due to a single level is $6\pi\lambda^2$, where λ is the de Broglie wavelength of the photon (20). For a 7 Mev. photon this is approximately 100 barns.

In any actual case this will be reduced by thermal Doppler broadening since the radiation widths Γ_γ at this energy of excitation are of the order of a few tenths of an electron volt (from neutron capture and scattering experiments) while the Doppler widths, δ , are of the order of 10 ev. ($A = 25$) depending on the atomic weight and temperature of the material. Hence the actual maximum value of the cross-section will be

$$\sigma_{\max}(\text{actual}) \doteq \sigma_{\max} \frac{\Gamma_\gamma}{\delta}$$

$$\sim 1 \text{ barn for } A = 25.$$

It must be stressed that this is of the order of 10^5 times the Thomson cross-section for the nucleus.

At this point in the discussion it becomes necessary to mention the inelastic scattering of photons by nuclei. This might well be called the Nuclear Raman Effect (21). In this case the nucleus is left in an excited state after the scattering and the energy of the scattered photon degraded correspondingly. This effect is small (21) except for highly deformed nuclei but its tendency will be to reduce slightly the elastic scattering cross-section.

At the threshold for (γ -N) and (γ -P) reactions the elastic scattering cross-section should drop due to

competition from particle emission. The inelastic events in this region correspond to photodisintegration in which some of the incident photon survives; a very unlikely process.

As the energy of excitation is further increased the correlation between nucleons begins to breakdown and the region of the dipole resonance is reached. The photon scattering should also show a peak here and the forward scattering amplitude would be derivable from a simple dispersion relation if the total absorption cross-section due to the various photo-nuclear reactions which take place in this region were adequately known.

Having very briefly outlined the low energy region, the region above 50 Mev. in which the author's own experimental work has been done will be examined in some detail.

The theory discussed below is based on several assumptions whose validity is ultimately determined by the fit of the theoretical predictions to the experimental values. If, however, some of the assumptions can be justified by appeal to independent evidence, then a good fit can be regarded as a more positive indication of the "truth" of the others.

To predict the scattering of photons of energy between 50 and 130 Mev. by nuclei three assumptions (22) (23) are necessary.

1. The nucleons can be regarded as free in intermediate states in this energy region.
2. The impulse approximation is valid.

3. Mesonic polarisation and anomalous moment effects can be neglected for energies almost up to meson photoproduction threshold. i.e. Almost Thomson scattering by protons and negligible scattering by neutrons.

With these assumptions the problem becomes almost exactly analogous to the scattering of soft X-rays by atoms. This scattering is known as Rayleigh scattering and is thoroughly treated by Compton and Allison in their book "X-rays in Theory and Experiment".

The first assumption however seems to have no theoretical justification and is the one the author's experiment sets out to test. It is very important for it implies that a nucleus, for example ${}^{16}_0$ would scatter photons like an assembly of 16 nucleons rather than an assembly of 4 alpha-particles or N other subgroups.

The use of the second assumption which largely follows from the first was for a long time a vexed question in the atomic case, but in the nuclear case it seems more justifiable. Adopting first elementary approach to the validity of the impulse approximation we note that the time taken for a photon to cross the nucleus is less than 10^{-23} seconds which is short compared with

the characteristic nuclear times which are $\sim 10^{-21}$ seconds. More formally this is equivalent to pointing out that nucleons can be treated non-relativistically unlike the electrons in heavy atoms.

The third assumption seems at first to be in direct contradiction of the first assumption. If the nucleons are to be regarded as free in intermediate states then they must scatter photons in the manner expected of ordinary nucleons. While it has been shown in the previous section that the mesonic polarizability contributed little to the cross-section in this region the effect of the anomalous moment could not be neglected. The solution lies in the fact that the anomalous moment scattering is spin dependent and in a detailed calculation Gomez (22) has shown that for nuclei in which the spins cancel, the anomalous scattering of the individual nucleons has little effect and even in other nuclei the anomalous part is small because of the coherence of the Thomson scattering.

If one is equipped with these assumptions, the calculation of the scattering cross-section for a nucleus containing Z protons is relatively simple. The method resembles one used in the solution of many of the problems of physical optics. The scattering amplitude due to the whole nucleus is obtained by a linear super-

position of the amplitudes from each proton due allowance being made for their relative phase.

The sum of the Z individual amplitudes gives, on squaring, the scattered intensity, I_z . In terms of the intensity due to one proton, I_p , it is given by (24)

$$I_z = I_p \left\{ Z + (Z^2 - Z) f^2 \right\}$$

where f^2 is the so-called nuclear form factor (of the electronic structure factor of atomic physics). f^2 depends on the distribution of protons in the nucleus, the wavelength, λ , of the radiation and the angle of scattering ϕ

$$f^2 = \left(\int_0^\infty u(a) \frac{\sin Ka}{Ka} da \right)^2$$

where $u(a)da$ is the probability that any particular proton lies between radii a and $a+da$ and K is a function of wavelength and angle of scattering given by

$$K = \frac{2 \sin \frac{\phi}{2}}{\lambda}$$

If I_z is written

$$I_z = I_p \left\{ Z^2 f^2 + Z(1 - f^2) \right\}$$

then the physical significance of the terms becomes apparent. It

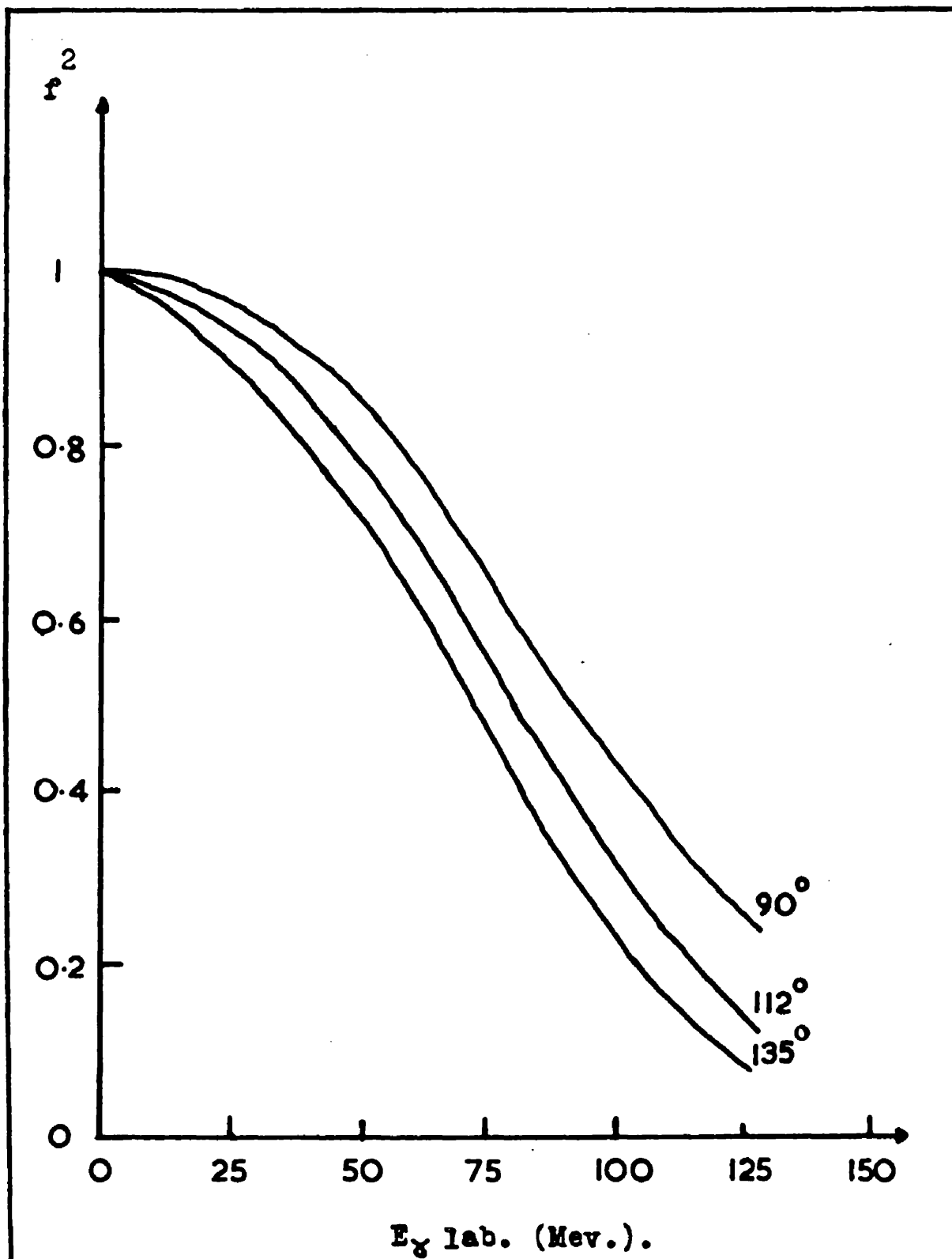


Fig. 6.

The Form Factor Evaluated for the C^{12} Nucleus.

is seen that the second term is proportional to Z and not to Z^2 , this corresponds to an addition of intensities not amplitudes and represents the incoherent or inelastic part of the scattering. (The modified radiation in the atomic case). However, since the experiment performed by the author makes no distinction between elastic and inelastic events the total I rather than the coherent (elastic) $\sum_P I Z^2 f^2$ will be used for comparison with experiment.

In fact $Z(1 - f^2)$ is probably an overestimate of the inelastic scattering since the number of final states of the nucleons is limited by the Pauli exclusion principle. It is difficult to estimate this effect but it probably reduces the inelastic scattering by a factor of about two.

The form factor f^2 depends on the choice of $u(a)$. In the particularly simple case where the protons are uniformly distributed in the nuclear volume, then $u(a)da$ has the form

$$u(a)da = \frac{3a^2 da}{R^3} \quad \text{for } a < R,$$

$$= 0 \quad \text{for } a > R,$$

where R is the nuclear radius. We take $R = 1.2 \times 10^{-13} A^{1/3} \text{ cm.}$

Performing the integration we have

$$f^2 = \left\{ \frac{3}{k^3 R^3} (\sin KR - KR \cos KR) \right\}^2.$$

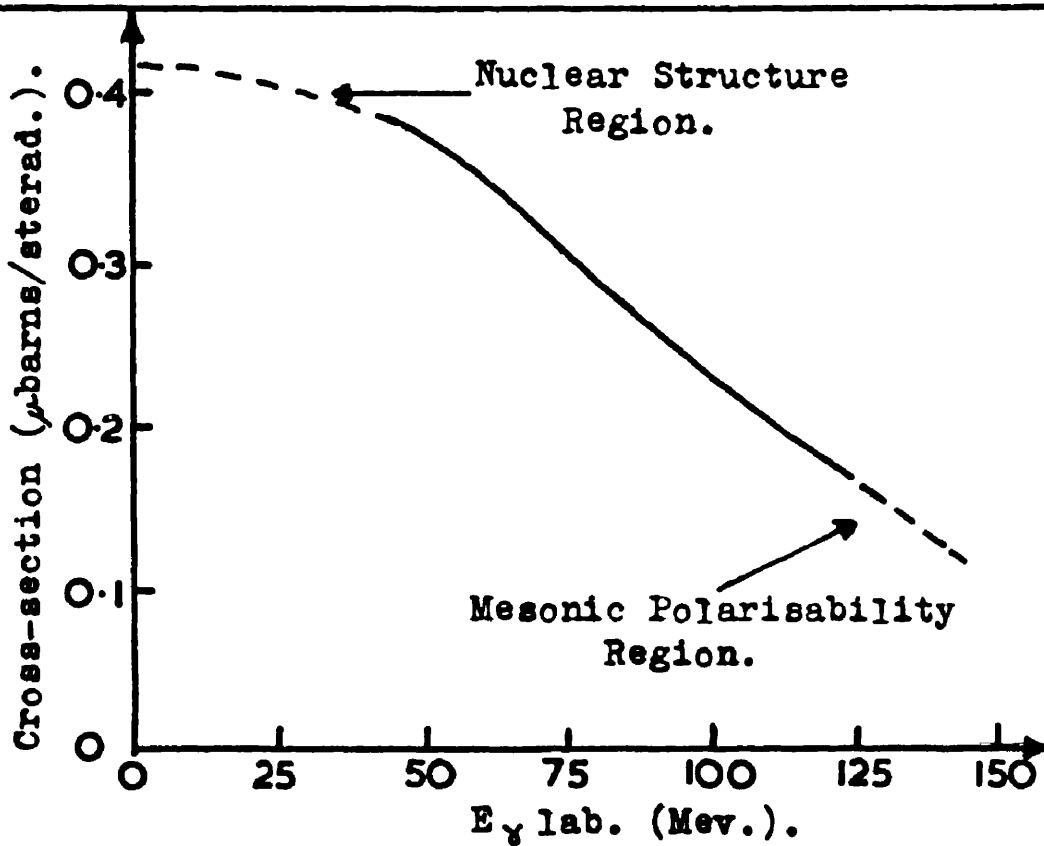


Fig. 7.

Predicted Scattering Cross-section at 90° .

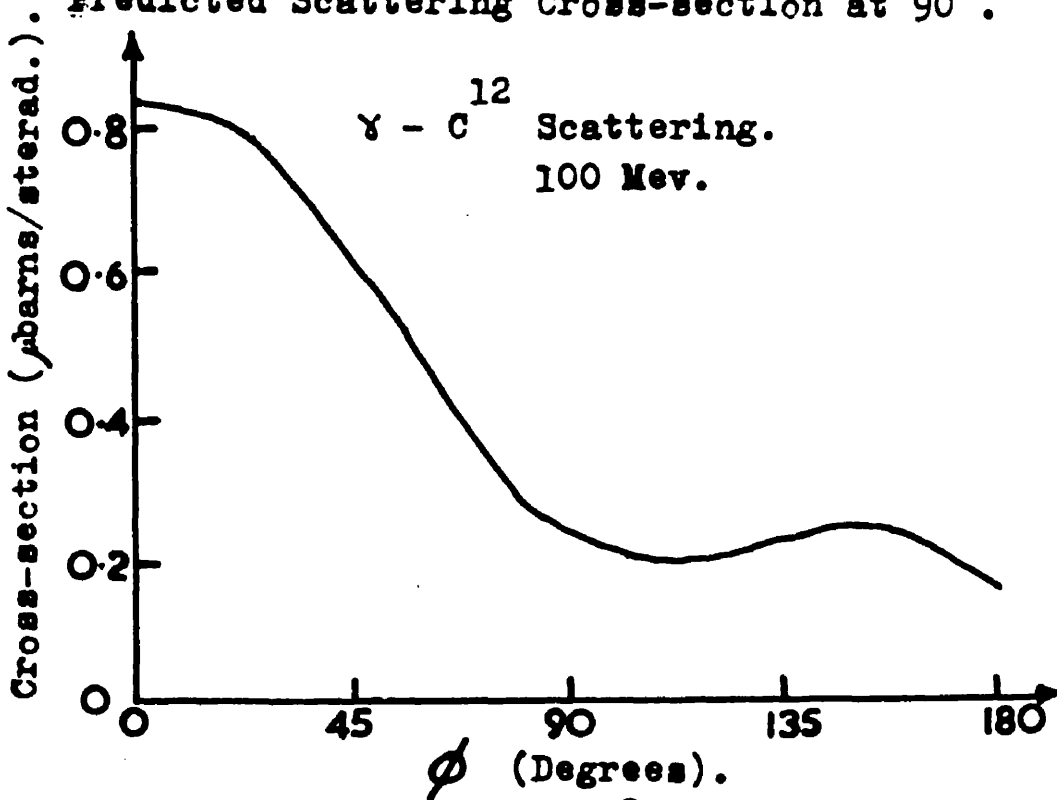


Fig. 8.

Predicted Angular Distribution.

This function evaluated for the C^{12} nucleus is plotted in Figure (6).

Returning for a moment to the validity of assumption (2), Brown and Woodward (25) have shown that the impulse approximation is valid in the atomic case if f^2 is not very small compared with unity. In the present case the lowest value of f^2 which occurs in the case of the largest momentum transfer corresponding to the scattering of a 130 Mev. photon through 135° is 0.075. Even this lowest value $\sim 1/13$ is probably only on the borderline of being called very small compared with unity.

The scattering cross-section expected at 90° on this model for the C^{12} nucleus is shown in Figure (7). The angular distribution expected at 100 Mev. is shown in Figure (8). The simple $1 + \cos^2 \phi$ of Thomson scattering is modified by the variation of f with angle. These are some of the curves with which the author's experimental points are compared near the end of this thesis.

Despite the fact that the assumptions on which this theory is based cease to be valid, it is instructive to look at the behaviour of its predictions at higher energy.

We note that as $k \rightarrow \infty$, $f^2 \rightarrow 0$. Thus $I \rightarrow \frac{ZI}{P}$. This implies physically that the cross-section for a nucleus of Z protons tends to Z times the cross-section for a single proton.

This is a satisfying result since it could have been predicted from a very general argument. When the wavelength of the incident radiation becomes very short compared with dimensions of the nucleus, the corresponding photon will tend to pick out the individual nucleons. Thus at very high energy the cross-section per nucleus will merely be the sum of the cross-sections of the individual protons and neutrons at that energy.

However in the region of immediate concern a little way above meson photoproduction threshold where there will be still some addition of different amplitudes no formal theoretical work has been done except for the deuteron. This is a special case since a wave-function has been deduced for this nucleus from the electron scattering experiments of Hofstadter. The lack of theoretical work on other complex nuclei is probably due to the fact that experimental investigation of this region is fraught with almost insurmountable difficulties.

SECTION 111Review of Previous Experimental Work.1. The Scattering of Photons by Protons.

The Proton Compton Effect is a two body process and therefore the measurement of the energy and angle of one of the products uniquely determines the interaction, including the energy of the incident photon if this is not already known.

The maximum energy of recoil of the proton from kinematical considerations is

$$T_{\max} = \frac{h\nu_0}{1 + \frac{M_p c^2}{h\nu_0}}$$

where $h\nu_0$ is the energy of the incident photon. At low photon energy this is too small to enable the proton to be readily detected and even at higher energy (at $h\nu_0 = 100$ Mev. $T_{\max} = 16$ Mev.) the necessity of measuring the proton energy imposes too great a restriction on the target thickness. Thus in the region up to meson photoproduction threshold all groups have made their measurements on the scattered photons.

To test the low energy limit of the scattering of photons by protons only one experiment has been performed. This was done by Alvarez, Crawford and Stevenson (26) (1958) who present their

results with an almost apologetic attitude which the present author thinks unwarranted. They state that they attempted the experiment because they thought mistakenly that some information about the meson field could be obtained. Nevertheless the results they obtain are of value since they confirm the theoretical predictions in this region. They scattered 1.6 Mev. photons from a radioactive source from LiH and Li to obtain the scattering from hydrogen by subtraction.

The main difficulty in the experiment is the very low cross-section: $\frac{d\sigma^p}{d\Omega}$ is only $1.55 \times 10^{-32} \text{ cm}^2/\text{sterad.}$ i.e. 15.5 millimicrobarns at 124° the angle at which the experiment was performed. The next difficulty is the background due to the ordinary Compton scattering of photons by the electrons of the target; a process several million times more probable than nuclear scattering.

The first difficulty was overcome by using an exceedingly strong source. It was 100 curies of ^{140}Ba --- ^{140}La , sixty per cent of whose radiation is 1.6 Mev. gamma-rays.

Their detector was a four-inch diameter four-inch high sodium iodide crystal viewed by a five-inch photomultiplier. This counter had sufficient energy resolution to allow the biasing out of counts due to the ordinary Compton effect in which the photon

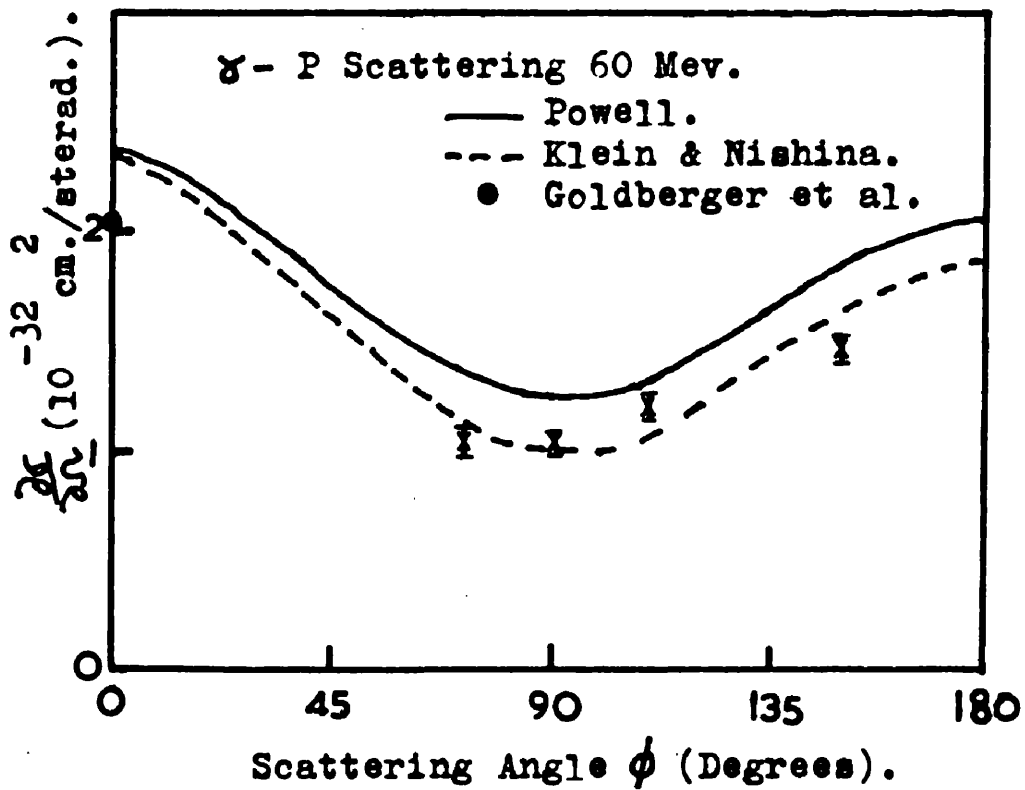


Fig. 9.

The Results of Oxley & Telegdi compared with the Predictions of Powell, Klein & Nishina and Goldberger et al.

energy is degraded.

The result they obtained was that the ratio of the observed cross-section to the classical Thomson cross-section was 0.96 ± 0.16 which is in agreement with the low energy field theoretic predictions (1).

In the energy range up to 25 Mev. no experimental results are available. This is perhaps due to the lack of theoretical interest in this region.

One point on the excitation function averaged between 25 and 87 Mev. has been determined by Oxley and Telegdi (27)(28) who scattered 87 Mev. bremsstrahlen from liquid hydrogen and used a photon sensitive counter telescope with low energy cut-off as detector.

They obtained the differential cross-sections shown in Figure (9). The dotted line is the Klein and Nishina formula and the full line corresponds to the predictions of Powell (5) including the effect of the anomalous magnetic moment. The point at 0° scattering angle is from the dispersion relations of Goldberger et al.(16). While these results cannot be said to support Powell's predictions, the ± 8 percent uncertainty in the absolute value of the experimental cross-sections (not shown), makes them not inconsistent with it.

The present author feels that when the problem is

considered physically doubtful is the case on the validity of Powell's treatment. If the anomalous part of the magnetic moment is attributed to the meson field and not to the core the magnetic moment observed by a photon during the very short time of interaction may be quite different from the "D.C." value used by Powell. Thus more experimental work in this region would be welcome.

The region up to meson photoproduction threshold has been investigated by two groups, Pugh et al. (23), in America and Govorkov et al. (29) in Russia.

The American group scattered 130 Mev. bremsstrahlen using a liquid hydrogen target. They identified the scattered photons by means of a scintillation counter telescope and measured their energy with a total absorption scintillation spectrometer.

They obtained several points on the excitation function[⊠] at each of the angles 45° , 90° and 135° . The results agree with either the Klein and Nishina formula or Powell except for the 45° data which were too high at the low energy end. The offending results were later withdrawn (15) and the corrected results transformed and interpolated to 90° in the centre of mass system are given in Figure (10).

Govorkov et al. have obtained one point on the excitation function at 100 Mev. Unfortunately the author has been unable to obtain a copy of the Russian journal in which

⊠ The term excitation function is here taken to be the variation of cross-section with energy.

this result is published and therefore can give no details of the technique used.

The next step upwards in energy involves a many fold multiplication of the difficulty of an already difficult experiment.

For photon energies above 130 Mev. photoproduction of real mesons at protons becomes energetically possible and these mesons decay almost immediately into two photons which are indistinguishable from scattered photons.

Thus as well as the Proton Compton Effect



there is



the cross-section for the second process being ~ 500 times greater than that for the first.

It is now necessary to detect the recoil protons and measure their energy as well as the scattered photons in order to distinguish between the two reactions. Detecting protons means that the target thickness must be reduced and hence the number of events per unit time drops sharply.

Bernardini et al. (30)(14) of Illinois are the only group to obtain any results in this region. They measured the energy and angle of the scattered photon with a total absorption

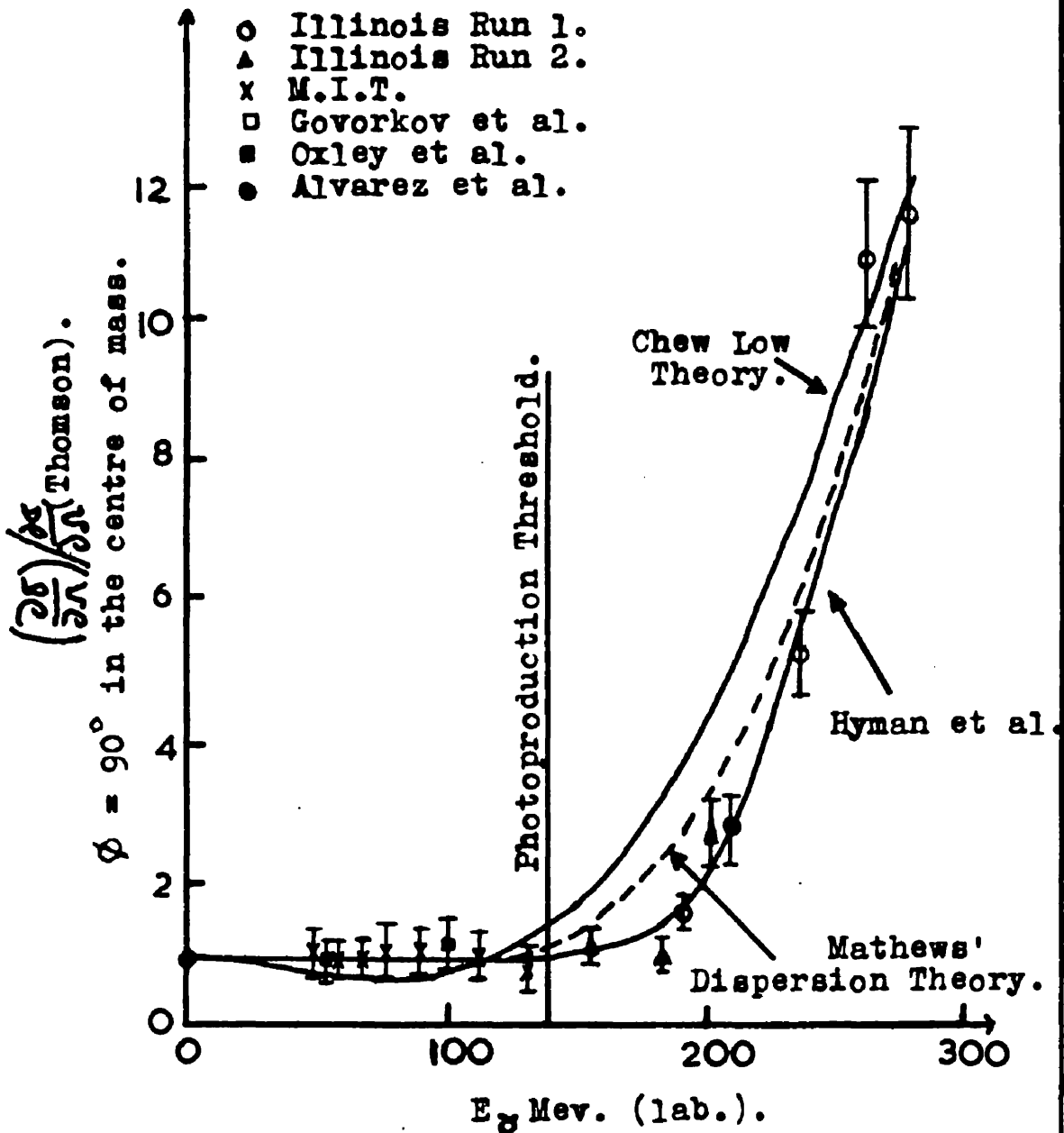


Fig. 10.

The Comparison of the Experimental Results
with the Best Theoretical Predictions.

Cerenkov spectrometer and derived the energy of the proton in coincidence from magnetic analysis, time of flight and dE/dx and E measurements made simultaneously.

Though no formal paper has appeared, the results obtained have been given in the reports of the various high energy conferences in the last few years. They are shown in Figure (7).

The solid line which fits the points well is the semi-phenomenological theory of Hyman et al. (15). However this type of theory is never very satisfying since one feels that if enough terms are involved (Hyman used 4 terms) almost any curve can be fitted. This is especially true in this case since the unknown π^0 lifetime is used as a free parameter. The Mathews' dispersion curve does not fit the points as well as it might look at first sight, since in the important region near pion photoproduction threshold the disagreement is nearly a factor of two. It has been pointed out (15), however, that the Mathews' curve was evaluated before the absorption due to the second isobaric state of the proton was known and its inclusion may improve the fit. The Chew Low calculation on the other hand seems to be well out, but as this theory is now suspect, it will not be considered further.

There is only one point the author would like to make, namely that the two experimental points at the high energy end of

the region seem to suggest that the top of the resonance may be at a lower energy than expected and the present work of the author (not included in this thesis) is an investigation of the Proton Compton Effect in this region. Littauer et al.(31) at Cornell and Kratz et al.(32) at G.E.C. are also working on this problem.

Above 350 Mev. the experiment becomes virtually impossible since the rest mass of the π^0 meson becomes a small part of the total energy of interaction and the kinematics of the two processes become similar. Further if the π^0 meson has appreciable momentum then the decay photon going in the same direction will have nearly all the energy of the π^0 , making the distinction between the two processes very marginal.

2. The Scattering of Photons by Complex Nuclei.

We use the established procedure of considering first the low energy region. Before discussing any actual experiment, in order to elucidate the difficulties involved in this region, the author would like to consider a hypothetical one. Suppose a beam of 2 Mev. photons is incident on a medium Z target and scattered photons are observed by means of a detector placed at 45° to the incident beam. The processes which can give counts in the detector are enumerated below. (After Burkhart (33)).

- 1) Compton scattering by "free" electrons.
- 2) Compton scattering by bound electrons.
- 3) Rayleigh scattering by bound electrons.
- 4) Raman scattering by bound electrons.
- 5) Thomson scattering by the nucleus.
- 6) Scattering by nuclear excitation.
- 7) Delbrück scattering by the nuclear Coulomb field.
- 8) Bremsstrahlen from photo-, pair or Compton electrons.
- 9) Annihilation radiation.

The effects of interest are of course the nuclear scattering (5) and (6); of the others some are small or can be eliminated by experimental techniques or their effect accurately evaluated, except for (3) and (7).

The calculation of Rayleigh scattering (34), (35), (25) and of Delbrück scattering (36), (37) has as yet yielded only qualitative results especially in the case of high momentum transfer (large angle scattering). These approximate theories predict that the Thomson and Rayleigh scattering amplitudes interfere constructively, while both interfere destructively with the Delbrück amplitude; however so long as quantitative predictions of these processes are lacking it seems impossible to abstract the nuclear scattering with any quantitative accuracy. Although there are these difficulties in interpretation the experiment in this region has been tackled by several groups, but for the light elements only one set of results is available.

Alvarez et al. (22) whose technique has already been described (^{See} ~~ibid.~~ p.20) measured the scattering from H, Li, C and Al nuclei. They obtained results in excellent agreement with the Thomson cross-section despite the considerations discussed previously. This is probably due to the fact that Rayleigh scattering varies as roughly the ninth power of Z (38) and Delbrück as the fourth power of Z (36), (37) hence the effects of these processes will appear more markedly for heavier elements.

The most complete experimental work in the low energy, high Z region has been done by Burkhardt (33) who gives many references to previous work. He measured the elastic scattering cross-

section between 0.5 and 3.0 Mev. using bremsstrahlen from a Van de Graff electron accelerator, all previous work having been done with radioactive sources. His detection system consisted of a NaI(Tl) scintillation counter shielded by absorbers. The output of the counter was fed into a ten channel kicksorter which was adjusted to register photons whose energy was more than eighty-five per cent of the peak energy of the bremsstrahlen and hence recording elastic scattering only. The experiment was attempted for Al but failed because of high background though results were obtained for Pb, In, Cd and Cu and despite the uncertainties in the analysis already mentioned gave some indication of the nuclear scattering. He concluded that as well as Thomson scattering there was scattering due to nuclear excitation.

As has been already mentioned, scattering of photons by nuclear levels is only effective if the photon has an energy almost exactly equal to the level energy within ~ 1 ev. Experiments measuring this resonant scattering have been carried out by Moon et al. (39), (40) and Malfors^m (41). These authors scattered photons from the decay of an excited state of some nuclide by means of a target of the same nuclear species. It was necessary, however, to make up for the recoil of the de-exciting nucleus. This was done by means of mechanical motion by Moon et al. and by thermal motion by Malfors^m to give the

required Doppler shift.

The resonant scattering was definitely observed and used to obtain level widths.

The extension of the experiment over the dipole resonance has been done by Fuller and Hayward (42) using radiation from a betatron. They give reference to the previous experiments using photons from nuclear reactions, e.g. Stearns (43) who scattered $\text{Li } (p, \gamma)$ photons.

They measured the scattering at 120° since in this energy region at backward angles Rayleigh and Delbrück scattering can be neglected. The technique adopted by these workers was similar to that of Burkhart, namely a NaI (Tl) scintillation spectrometer operated at high bias to detect the photons scattered from the top of the bremsstrahlung beam. Moving the peak machine energy up in steps they obtained the excitation function for the process for several elements between Na and U. As predicted, the cross-section rose with increasing energy until particle emission threshold was reached, when it suffered a sharp drop. Above the threshold the cross-section rose again to a maximum corresponding to the dipole resonance. Fuller et al. found that for heavy nuclei the excitation function followed the (γ, n) giant resonance but for lighter nuclei the peak was at higher energy and broader. The maximum energy in the above experiment was 40 Mev. and up to this

point, as shown, there is good agreement between theory and experiment.

The energy region from 50 to meson photoproduction threshold (~ 130 Mev.) is the one in which the author's own work has been done and here there was a disagreement of a factor of between two and three between theory and experiment.

Scattering in this region was first observed by Pugh, Frisch and Gomez (44) of the Massachusetts Institute of Technology in 1954. In 1955 these authors reported (45) cross-sections between two and three times less than expected. It was this disagreement which induced Dr. W.S.C. Williams and the author to attempt the experiment. In 1956 work was started on the scattering from carbon and results were eventually obtained in good agreement with the theoretical predictions, but during the progress of this work the M.I.T. group published a very thorough paper (23) including the excitation functions for several elements now in agreement with the expected values.

In retrospect, after considering the difficulties of obtaining an absolute cross-section experienced here and also in M.I.T., confirmation of the values by another group was certainly needed.

As might be expected the two experimental set-ups were very similar. The most important difference lay in the

detector for the scattered photons. Pugh et al. used a scintillation spectrometer while the present author used a Cerenkov spectrometer. This represented an advance in technique since Cerenkov counters are noted for their insensitivity to background radiation. This enabled the counter to be operated with a thinner filter in front of it. The thick filter used by the M.I.T. group nearly had a disastrous effect, as it was their results at 45°, at least the low energy ones, were rendered valueless. Another difference between the two experiments lay in the coincidence telescope used to identify the scattered photons. The initial Glasgow runs were done with a rather poor geometry telescope but the difficulties this introduced made clear the requirements of a good system and this was built for the second series of runs in which the absolute cross-section was obtained. The telescope used by the M.I.T. group in all their runs was of intermediate merit.

To complete this review, the energy region above meson photoproduction threshold must be mentioned. As yet no experimental work has been done on complex nuclei in this region, not even deuterium. The scattering from this nucleus would be of great interest as the nearest approach to the scattering by a free neutron. The fact that the deuteron has no bound excited states makes this experiment just possible. The problem is

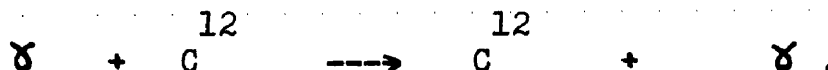
similar to that encountered in the investigation of the Proton Compton Effect in this region (^{See} *ibid.* p.23) the photoproduction of π^0 mesons, only the recoiling particles would have to be identified as a deuteron and its energy measured in this case. This would give the elastic scattering, the inelastic scattering could not be distinguished from inelastic π^0 photoproduction both being three body processes.

With present techniques the investigations of the elastic scattering from higher Z nuclei is impossible for not only would the recoiling nucleus have to be identified as (Z, A) and not say (Z, A-1), it would have to be verified that it was not in an excited state. Such investigations might become feasible if monochromatic photon beams became available.

CHAPTER 11.THE INSTRUMENTATION OF THE PHOTON SCATTERING EXPERIMENT.SECTION 1.The Experimental Requirements.

Before discussing the instrumentation in detail the author would like to recapitulate briefly some general considerations.

The reaction investigated by the author was



As stated before the measurement of the energy and angle of one of the products uniquely determines the interaction, including the energy of the incident photon out of the bremsstrahlen which would not otherwise be known. The low cross-section demands a thick target and therefore rules out any possibility of making measurements on the recoiling nucleus. Thus an energy sensitive photon detector is required, preferably one of high efficiency and capable of subtending a large solid angle at the target. These second requirements ruled out the possibility of using a pair spectrometer as detector. Therefore, at the expense of energy resolution, it was necessary to fall back on the class of detectors known as total absorption spectrometers. The operation of this

type of device will be discussed in detail later.

The other requirements of the experiment are the angle and identity of the scattered radiation. To fulfil this need the photon sensitive scintillation counter telescope described in Section III was used.

The integration of these two parts into a single unit to measure the energy and angle of the scattered photon required a considerable amount of electronic circuitry. This is treated in Section IV.

SECTION 11.

The Cerenkov Total Absorption Spectrometer.

1. The Construction of the Spectrometer.

The interaction of a high energy photon or electron with matter is to produce a shower by the cascade processes of pair production and bremsstrahlung. In a total absorption spectrometer, as its name implies, as much of this shower as possible is retained within an absorber and to maintain reasonable dimensions this must be a material of high atomic number and high density (i.e. short cascade length).

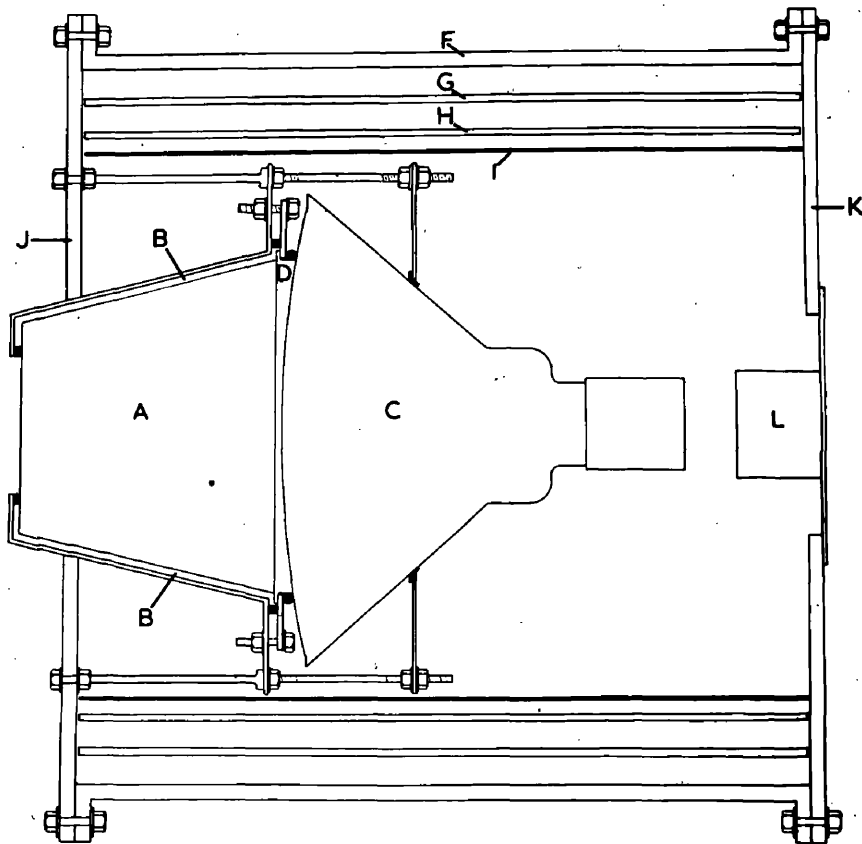
The ideal method of measuring the energy of the shower and hence the energy of the incident photon or electron would be a block of heavy scintillating material like sodium iodide viewed by a photomultiplier, however the size of block required is at present prohibitive. For ninety per cent capture of the shower (46) produced by an 185 Mev. electron, the sodium iodide crystal would have to be a cylinder ten inches in diameter and ten inches high for particles incident axially.

Liquid scintillators are of course available but since these are all "light" the dimensions become huge and light collection and background problems become serious. The M.I.T. group used a total absorption spectrometer of this type but the Glasgow group had previously considered it impractical.

Thus having rejected scintillators it was necessary to fall back on the Cerenkov Effect (47). Cerenkov radiation is emitted by a charged particle travelling in a transparent medium of refractive index, n , if its velocity, $v > \frac{c}{n}$, where c is the velocity of light in free space. Thus if a shower is developed in a transparent material Cerenkov light will be emitted by the relativistic electrons and positrons passing through the medium. The amount of light is proportional to the total relativistic track length of these particles and therefore the average amount increases monotonically with increasing incident energy, assuming that the fraction of the shower trapped remains constant.

Materials which have been used as absorbers include lead glass, Cassels et al.(48), carbon tetrachloride, Jones et al.(49), thallos chloride, Moffat and Stringfellow (50) and lead fluoride, Williams and Caplan (51).

The lead fluoride spectrometer built by Dr. Williams and the author unfortunately had too poor energy resolution to be suitable for the photon scattering experiment. This constituted a major experimental setback, but the author applied the experience gained from the lead fluoride instrument to the construction of a similar spectrometer using lead glass as absorber. This spectrometer in its final form is described below.



- A Lead Glass Absorber.
- B Magnesium Oxide.
- C 15" Dumont Phototube.
- D Perspex Lens.
- F - H Steel Magnetic Screens.
- I Mu-metal Magnetic Screen.
- J & K Steel Supporting Discs.
- L Electronic Accessories.

Figure 11.

Diagrammatic View of the Cerenkov Spectrometer.

The lead glass absorber is in the form of a truncated cone, $7\frac{1}{2}$ inches diameter expanding to twelve inches in diameter and nine inches high. Since in this glass the cascade length is one inch these figures also give the dimensions in this unit. The block was mounted with its axis horizontal and was viewed, at the twelve inch end, through a perspex light guide in the form of a plano-concave lens by a Dumont fifteen inch phototube type K1258, as shown in Figure (11).

Light collection is a very important factor in Cerenkov spectrometers, since very much less light is obtained from the Cerenkov Effect than is obtained from scintillation. It was found experimentally that a 0.5 Mev. electron in NaI(Th) gave as much light as a 50 Mev. shower in the lead glass. Indeed the ~~optical~~^{con} shape of the absorber is only to retain, by total internal reflection, some light that would otherwise be lost. The light collection was also further improved by using liquids to create optical contact between the various parts of the system. Silicone oil was used between the plane surfaces of the glass and perspex, while between the concave surface of the lens and the convex surface of the phototube contact was made with paraffin oil. In order to regain some of the light which may escape, the glass was mounted in magnesium oxide. Figure (11).

With a fifteen inch phototube magnetic screening is

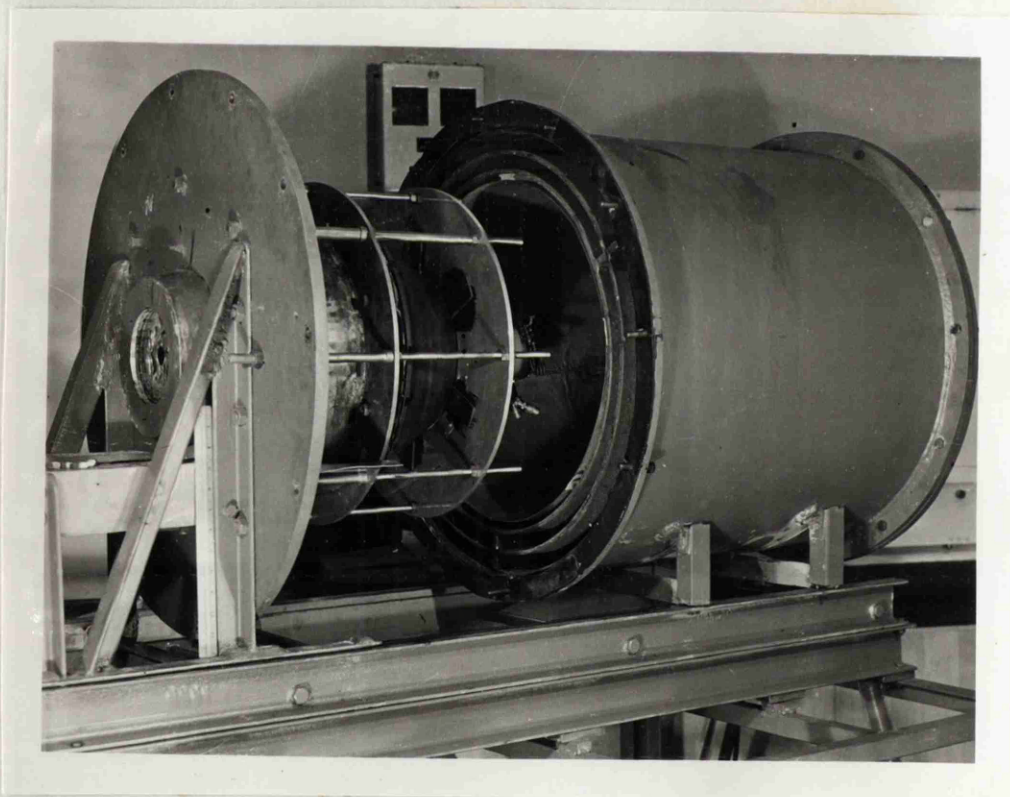


Figure 12

View of the Cerenkov Spectrometer Showing
the Magnetic Screening

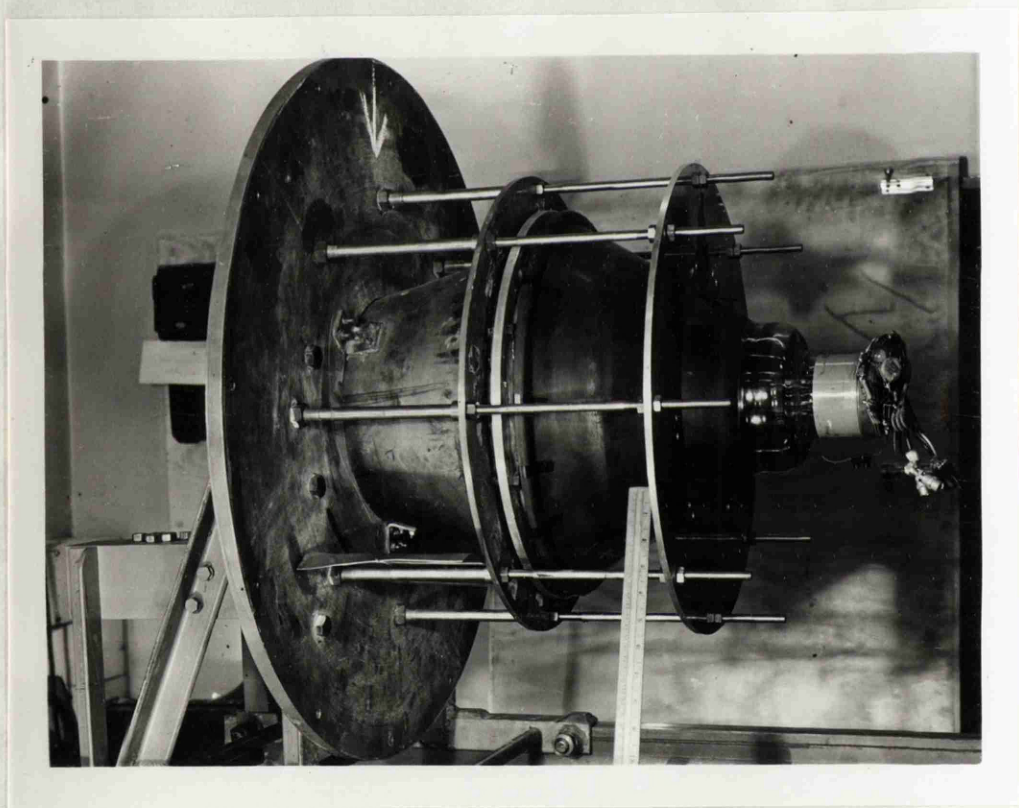


Figure 13

View of the Cerenkov Spectrometer
Showing the Construction.

vitaly important, since the photoelectrons emitted by the photocathode must travel nearly 30 c.m. to reach the first multiplying dynode with an average energy of only a few hundred electron volts. The stray magnetic field in the synchrotron beam room is of the order of a few gauss, due to the fringing fields of bending magnets and the fields due to the steel frame of the building. The magnetic screening used consists of three quarter inch thick coaxial steel cylinders and one 1/16 inch mu-metal, as shown in Figure (12). The field inside the screening, measured with a large flip coil, was ~ 25 milligauss when the outside field was one gauss.

The only practical difficulty experienced in the construction was the sealing of the optical contact liquid between the phototube and lens. Eventually the seal was made by pressing the fifteen inch photocathode against a soft foam rubber gasket. Another view of the spectrometer removed from its screening is given in Figure (13).

2. The Testing of the Spectrometer.

Since a total absorption spectrometer measures the energy of the electron photon shower produced, its response is virtually independent of whether the incident energy was in the form of an electron or photon. This enables the instrument to be tested and calibrated using a beam of monoenergetic electrons. (The derivation of this beam will be discussed in detail in the next section). The electron beam was passed axially through a counter telescope into the lead glass and the output of the spectrometer gated by the coincidence telescope was displayed on a hundred channel kicksorter as described in the next section.

The spectrometer was made to operate satisfactorily when the characteristics of the phototube were properly understood. It was found that the gain and noise of the tube varied sharply with the cathode first dynode potential and an optimum value was found. More important the electron collection and hence the resolution of the instrument depended critically on the potential of the electrostatic screen between the cathode and the first multiplying dynode. This is perhaps not surprising when the large distance between these electrodes is taken into account. An optimum value of this parameter was obtained by comparing the results of ten different settings.

All free parameters having been set, the necessary

electronic adjustments were made.

One other series of tests was made before the spectrometer was properly calibrated for the scattering experiment. Since the spectrometer was to be placed near a target from which photons would radiate, its response had to be checked for angular and non-axial entry of radiation. This was done and the differences of pulse height and resolution were found to be negligible within wide limits.

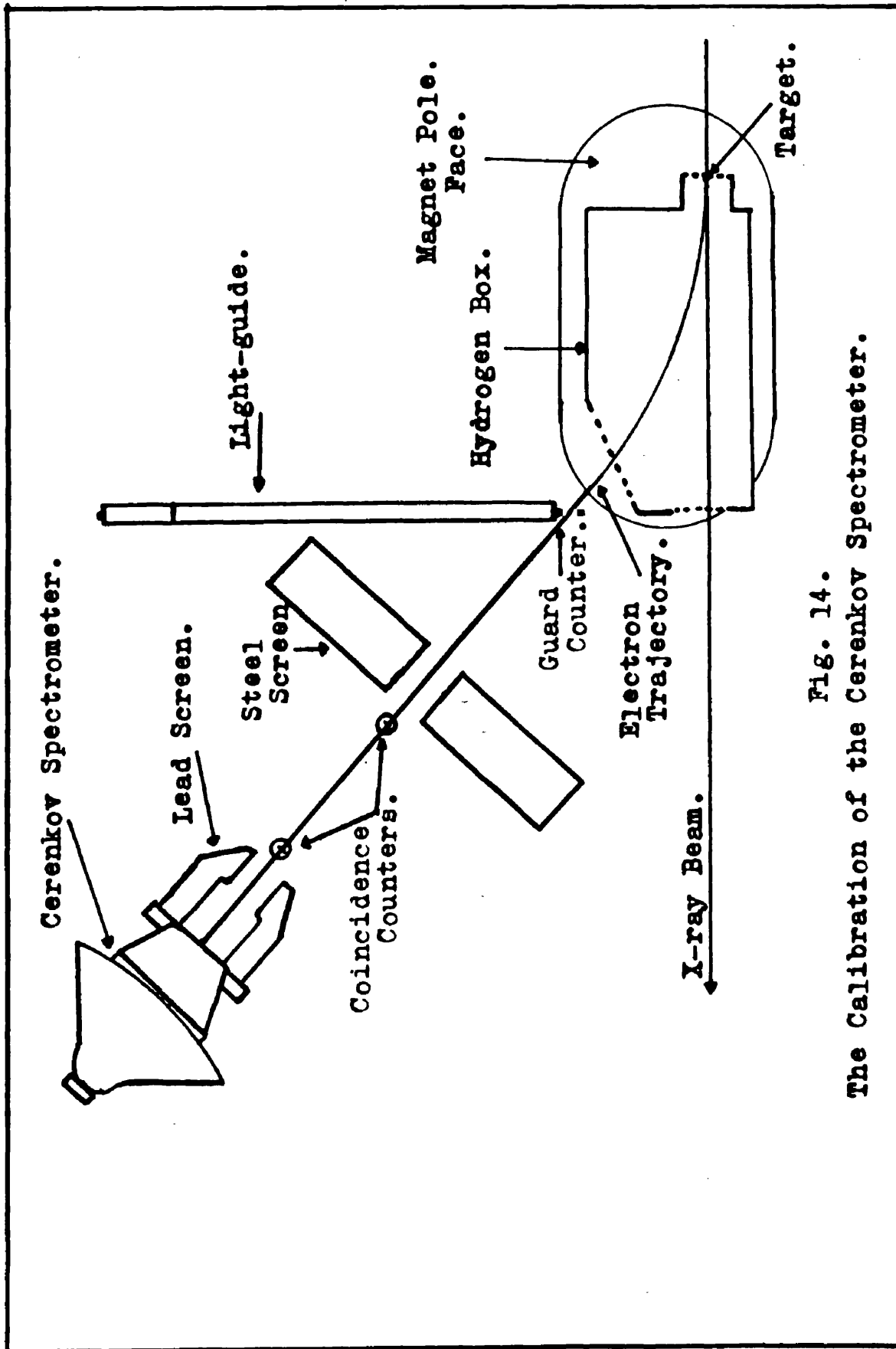


Fig. 14.
The Calibration of the Cerenkov Spectrometer.

3. The Calibration of the Spectrometer.

As stated before the spectrometer was calibrated using a beam of monoenergetic electrons. This beam was derived from magnetic analysis of the electron-positron pairs produced by the bremsstrahlen of the synchrotron, in a thin copper target placed between the poles of a large electromagnet, as described below.

An electron trajectory was determined and calibrated using a loaded current carrying wire as an analogue. A scintillation counter telescope and the Cerenkov spectrometer were moved into line with this trajectory outside the magnet. To reduce multiple scattering of the electrons and pair creation in the air, a copper box with the necessary thin windows and filled with hydrogen gas was placed between the poles of the magnet. The beam entry port of the box was made to coincide with the predetermined position of the target and the 5/1000 inch copper target was fixed against the window. The experimental layout is shown in Figure (14).

The scintillation counter telescope consisted of a guard counter (counter with a hole in the scintillator) and two ordinary scintillation counters operating in ACC. The two coincidence counters consisted of RCA 6810A photomultipliers viewing pieces of plastic scintillator, $\frac{1}{2}$ " across and 1" high. The first was $\frac{1}{8}$ " thick and the second, which is nearest the spectrometer was $\frac{1}{4}$ " thick.

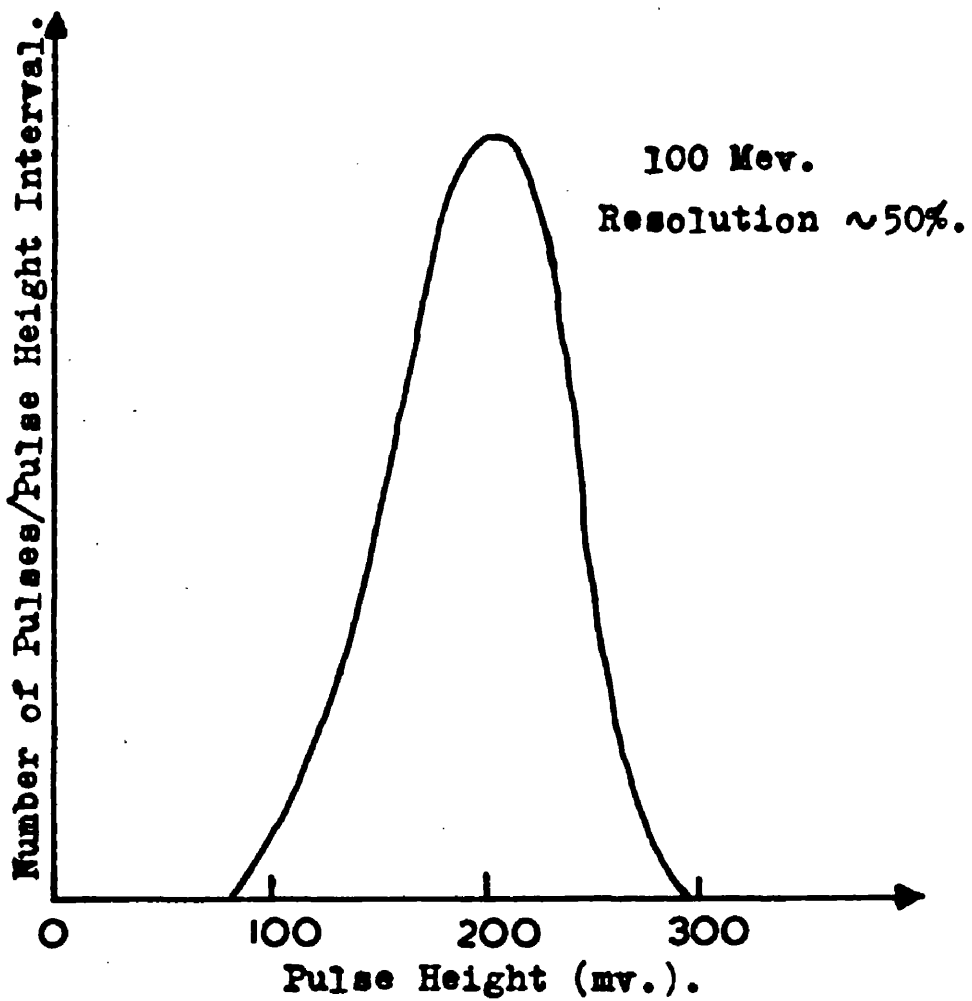


Fig. 15.

The Response of the Cerenkov Spectrometer
to 100 Mev. Electrons.

The guard counter merits description in a little more detail. The plastic scintillator was three inches by two inches $\times \frac{1}{4}$ " thick and had a hole three-quarters of an inch high and half an inch across cut in the centre of it. As this counter was designed to operate in the fringing field of the magnet and since ordinary phototubes will not operate in even a weak magnetic field a long light-guide was needed. This consisted of a one metre length of two inch diameter perspex rod wrapped in aluminium foil. The merit of this type of counter is that it verifies that the coincidence between counters (2) and (3) was due to an electron which passed down the calibrated trajectory without disturbing that electron's motion by multiple scattering.

An ACC signal from the telescope caused the amplified pulse from the Cerenkov spectrometer to be displayed on a 100 channel kicksorter. (Note - This was the final form of the electronics. Before the arrival of the high quality kicksorter, the pulses were displayed on an oscilloscope and photographed. However the electronics will not be discussed in detail here to avoid duplication later).

Four calibration runs were performed at magnet currents corresponding to 50, 100, 150 and 200 Mev. electron energy. Each run lasted about one hour during which time 5,000 counts were amassed on the kicksorter. A typical resolution curve taken at

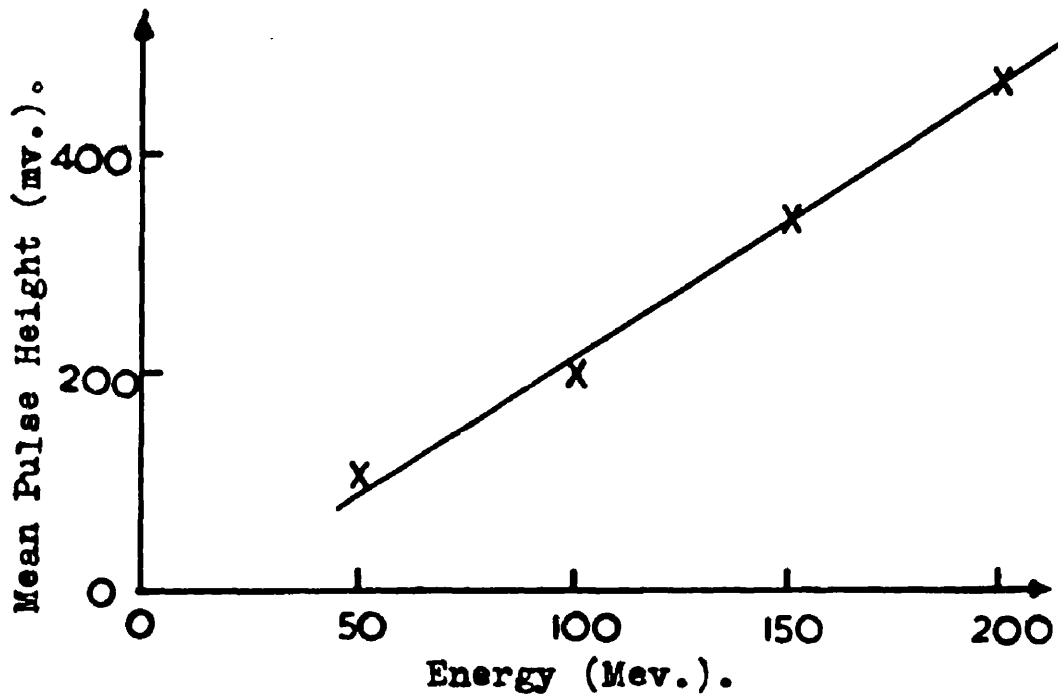


Fig. 16.

Variation of Mean Pulse Height with Energy.

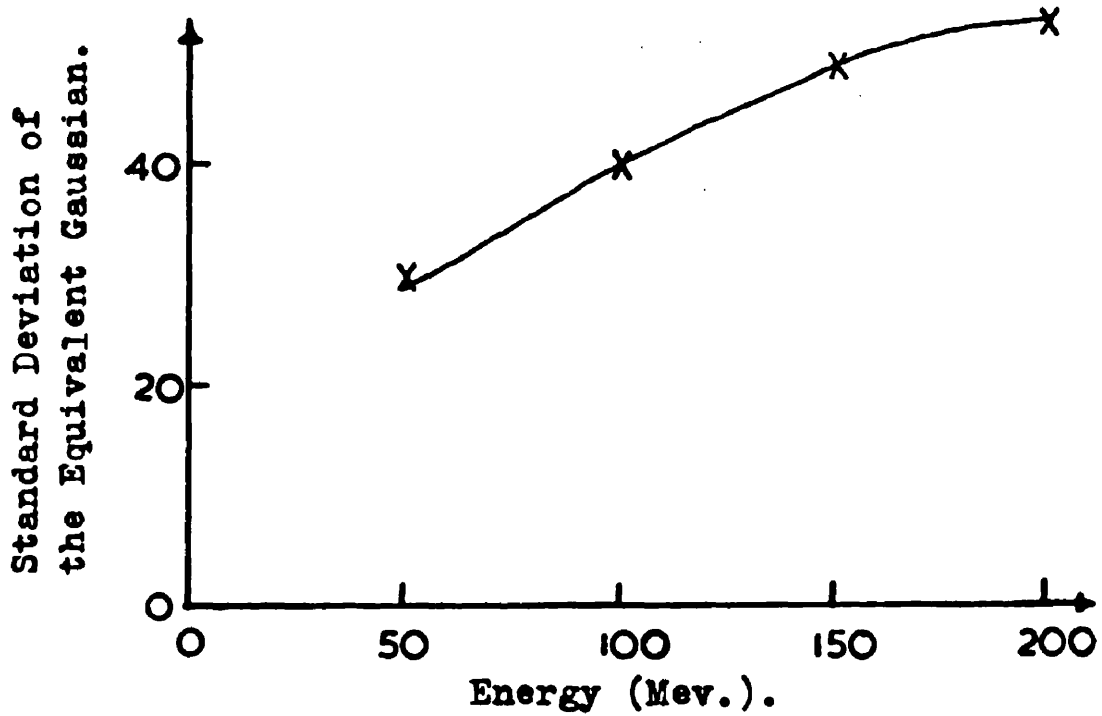


Fig. 17.

Variation of Resolution with Energy.

100 Mev. is shown in Figure (15).

The calibration runs gave two graphs necessary for the use of the spectrometer in an experiment.

- 1) Mean pulse height vs Energy, Figure (16).
- 2) Resolution (% full width at half height vs Energy, Figure (17)).

The absolute calibration having been obtained it was necessary to have some day to day means of checking its constancy. The following methods were employed:

- 1) An encapsulated half-inch NaI(Tl) crystal was placed in contact with the lead glass and exposed to the 1/2 Mev. positron annihilation radiation from a Na²² source. The pulses from the phototube were amplified and displayed on the kicksorter and the constancy of the position of the photoelectric peak was noted.

- 2) The background pulses in the Cerenkov spectrometer due to cosmic rays were displayed on the kicksorter. The spectrum took the form of a plateau followed by an edge and the position of half height on this edge was noted.

- 3) The third method measured the constancy of the electronics only and not the constancy of the phototube. In this case constant height pulses from a simple but carefully built pulse generator were injected through a variable attenuator into the anode of the phototube. By altering the attenuation the

linearity and gain could be checked.

It must however be stressed that though these tests were made regularly, no appreciable change in the characteristics of the Cerenkov spectrometer or electronics was found at any time.

The author feels that this fact may be added to the advantage of Cerenkov devices over large liquid scintillation counters which tend to be temperature sensitive.

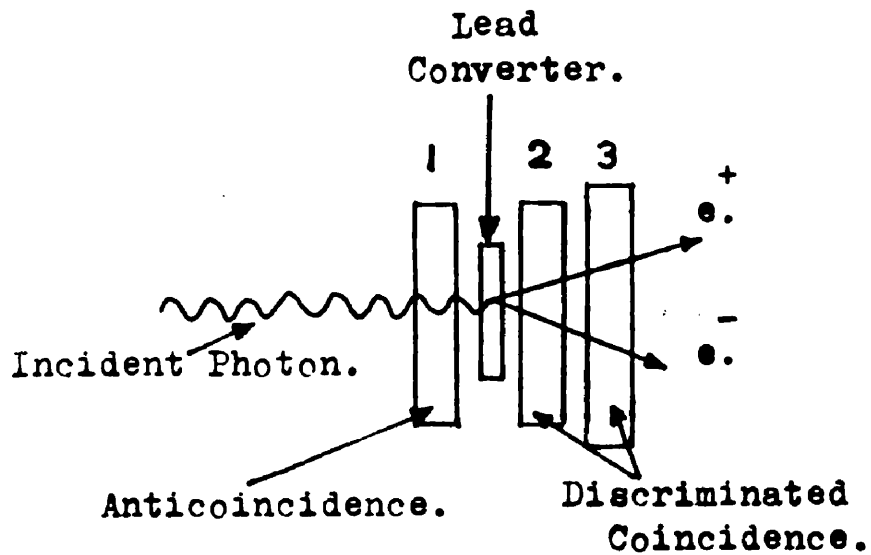


Fig. 18.

A Photon Sensitive Scintillation Counter Telescope.

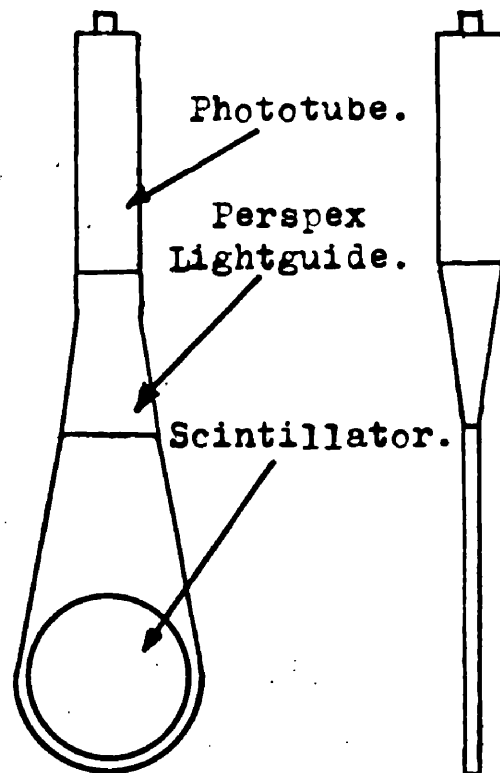


Fig. 19.

The Construction of the Scintillation Counters.

SECTION 111.

The Scintillation Counter Telescope.

1. The Purpose and Principle of Operation.

To avoid confusion, it must be stressed at the outset, that the counter telescope described in this section is in no way related to the device used in the calibration of the Cerenkov spectrometer treated in the previous section.

The present scintillation counter telescope forms an integral part of the detection system used in the photon scattering experiment. Its purpose is to identify those pulses observed in the Cerenkov spectrometer which are due to a high energy photon from the target. Figure (23).

The principle of operation is made clear by Figure (18). The photon to be detected passes through counter (1) and converts into an electron-positron pair in the sheet of lead, known as the converter. This pair then passes through counters (2) and (3). The electronic circuitry associated with the telescope is designed to respond to events in which there is no pulse from counter (1) and TWO electron pulses from each of counters (2) and (3) in coincidence.

In the actual scattering experiment the pair passes out of the telescope into the Cerenkov spectrometer, where its energy is measured. Figure (23).

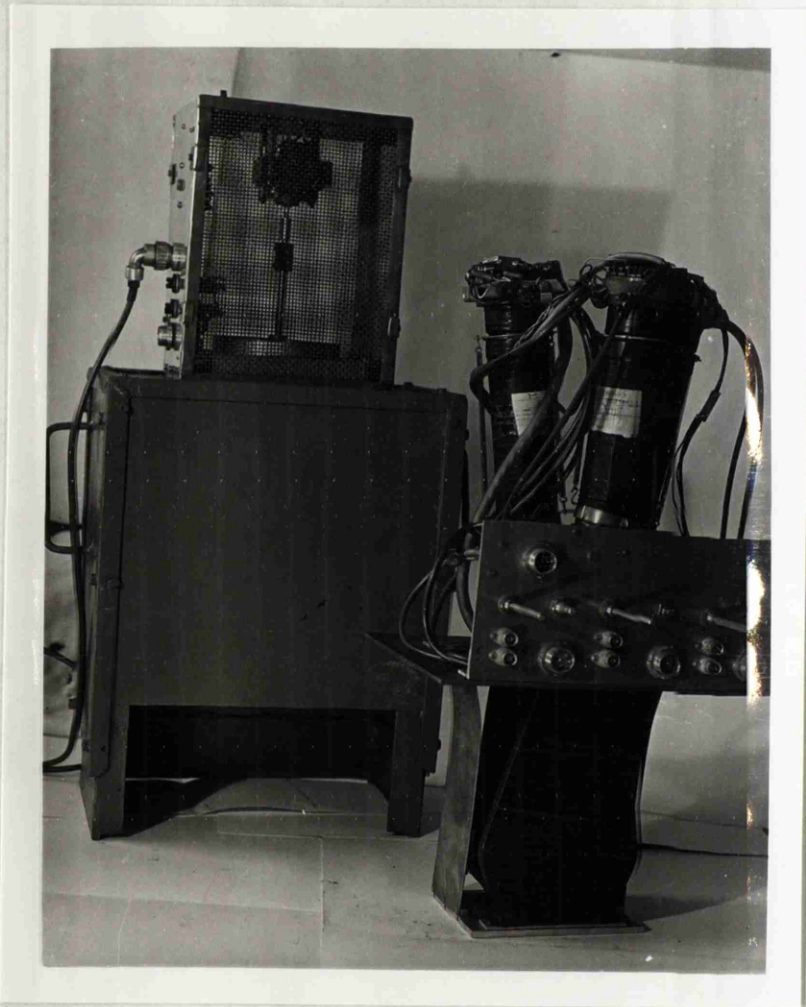


Figure 20

The Coincidence Telescope, Magnetic
Screening and Cooling Fan.

2. The Construction and Testing.

For the photon scattering experiment large solid angles are necessary. This means that the coincidence telescope must be large but very compact. The counters (1), (2) and (3) were therefore made up as shown in Figure (19) with the scintillators mounted in slim perspex light-guides. The plastic scintillators were $4\frac{1}{2}$ inches in diameter for counters (1) and (2) and five inches for counter (3) each being $\frac{3}{8}$ inches thick. These were shrink fitted into the perspex light-guides with a thin film of silicone grease as optical contact. To improve light collection the scintillators and light-guides were wrapped in aluminium foil. The RCA 6810 phototubes which viewed the scintillators were pressed against the light-guides with springs; optical contact being once again made with silicone grease. The phototubes were wrapped in aluminium foil connected to the photocathode to (-2.1 kV) reduce noise in the tube. Each assembly was then wrapped in two layers of Lassovic tape to make it light-tight and safe to handle. Each counter was then slipped into its position in the counter tray and fixed. The final assembly is shown in Figure (20).

In the scattering experiment these counters are mounted close to a thick graphite target in the X-ray beam and therefore the counting rate due to low energy electrons and soft photons

is very high. This means that the mean direct current through the tubes during the beam is high and hence to keep the multiplying dynode potentials constant the current through the associated resistor chain must be large. In the present case 5.6 ma. was used; this is about ten times the usual value. Incidentally this made necessary the installation of a cooling fan in the magnetic screen.

Two pulses were taken from each tube, a negative one from the collector and a positive one from the last dynode. These pulses were adjusted to the desired size by varying the E.H.T. voltage on the tube. This value varied slightly from tube to tube but was about 2,100 volts.

Before they could be used the counters had to be checked for saturation. This was done using Na²² and Co⁶⁰ gamma-ray sources. The energies of these gammas are 0.5 Mev. (annihilation radiation) and 1.15 and 1.33 Mev. and they give rise to electrons of maximum energy (Compton edge) of about 0.33 and 1.0 Mev. i.e. the maximum pulse height from Na²² annihilation radiation to the maximum pulse height from Co⁶⁰ is as 1:3 approximately. This provides a means for testing for saturation. However, since an electron-positron pair of total energy 100 Mev. will lose about five Mev. in the crystal, the voltage on the counters had to be raised to the maximum specified by the manu-

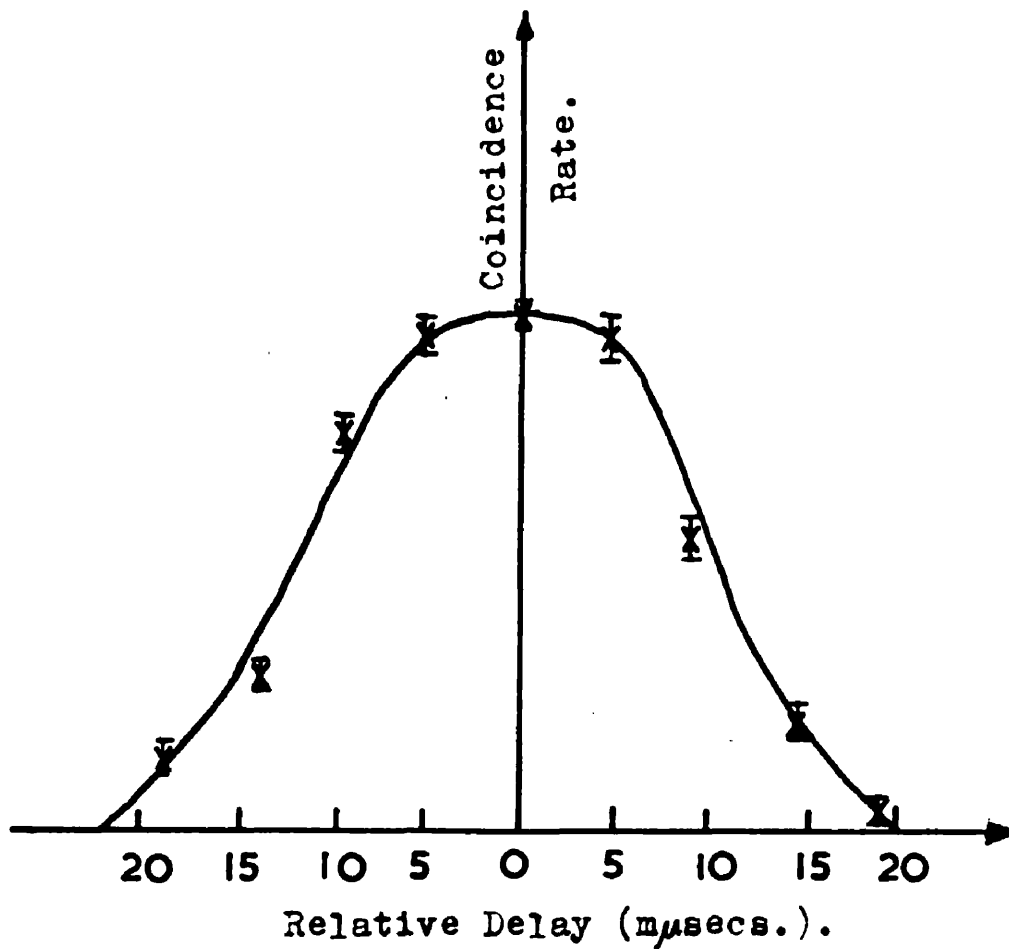


Fig. 21.

Curve Indicating the Equality of Transit Time
of Two Phototubes.

facturers (2.3 kV) to obtain the corresponding pulse height. No trace of saturation was found.

Tests for saturation were also made using cosmic rays. The counter under test was bracketed by two other scintillation counters one placed above and the other below. When a coincidence occurred between the two outer counters the pulse from the centre one was displayed on an Tektronix 517 oscilloscope and photographed. These events generally corresponded to cosmic ray μ -mesons passing through all three counters. The mean pulse height obtained was compared with the predicted value and no sign of saturation was found.

Before the three counters of the telescope could be used together their relative transit times had to be compared. This is to make sure that the pulses from the phototubes due to coincident events in the scintillators reached the coincidence circuit at the same time. To do this cosmic ray μ -mesons were again used. The counters were tested in pairs, one being placed a few inches above the other. The coincidence rate was then measured; an extra metre of cable was then put in the lead from one counter and the coincidence rate measured once more; this was repeated for lengths up to four metres extra on either side. The type of curve obtained is shown in Figure (21). This curve is almost symmetrical about the origin shewing that the

maximum counting rate occurs when there is no relative delay, i.e. the transit times of the two tubes are the same. This was found to be the case with all the tubes and no compensation was necessary.

Having described the counters the next part of the telescope to be treated is the converter. While the efficiency of a total absorption spectrometer is very close to 100 per cent for photons over 20 Mev., when this is used in conjunction with a counter telescope the efficiency of the detection system is determined by the converter. This efficiency increases with increasing converter thickness but so does the mean energy loss of the pair produced, hence a compromise must be reached. In the first set of runs the converter thickness was $\frac{1}{4}$ " of lead; while in the second set, designed to give the absolute cross-sections, an $\frac{1}{8}$ " converter was used. In the second case the converter was in the form of a three-inch disc mounted in a perspex holder slipped between counters (1) and (2). In the first case it was somewhat larger.

The detailed discussion of the behaviour of the telescope as a function of energy is given in the analysis section of this thesis, where the efficiency of the detection system is treated at some length.

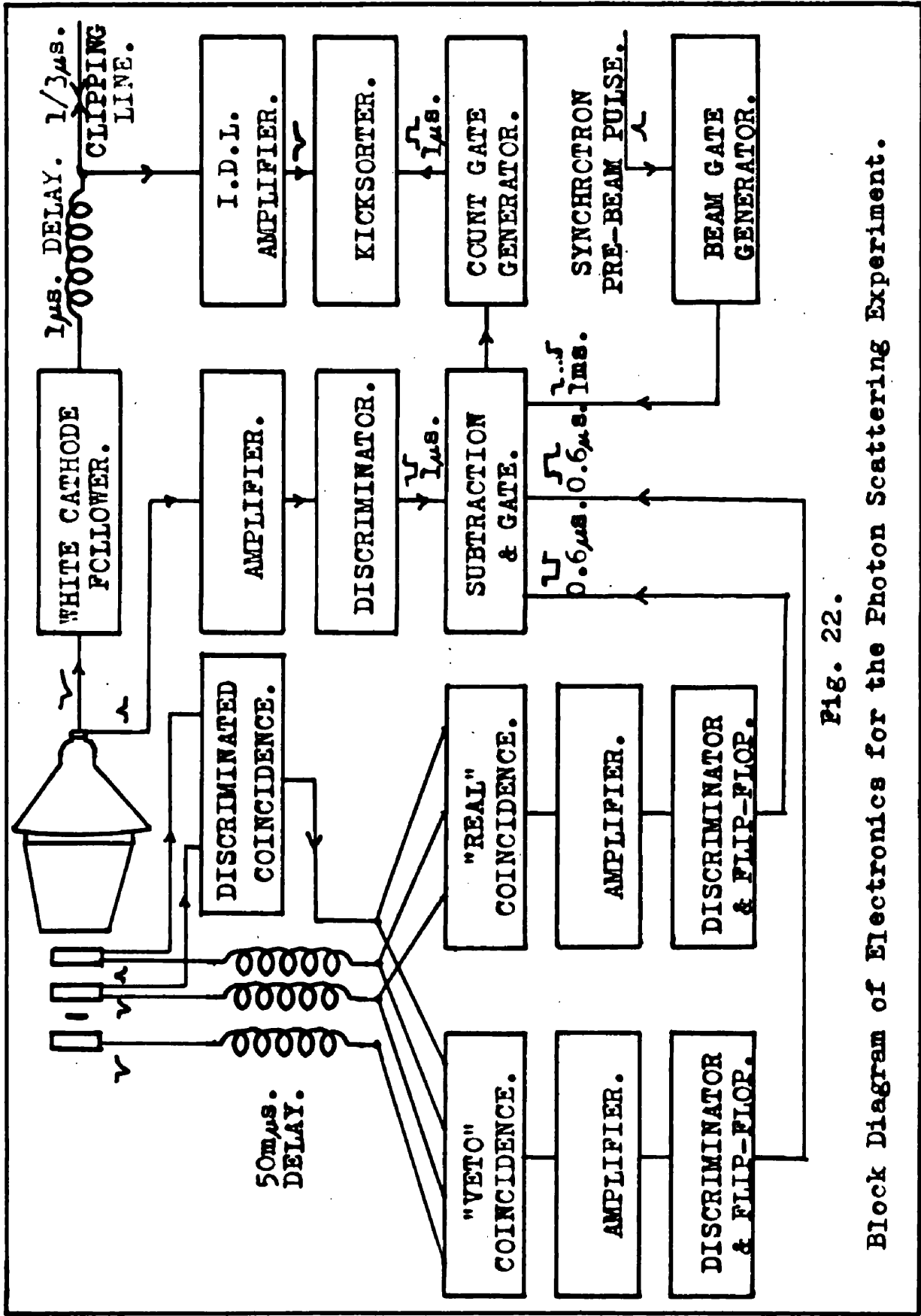


Fig. 22.

Block Diagram of Electronics for the Photon Scattering Experiment.

SECTION IV.

The Electronic Circuitry.

The main difficulties were associated with the counter telescope, in particular the anticoincidence. Due to its proximity to the beam (Figure 23) the counting rate in the anticoincidence counter was very high and no anticoincidence circuit tried, could be made to work effectively. The first step in overcoming this difficulty was putting 2" of graphite between the target and this counter as a filter to remove low energy photons and electrons. This meant the loss of ten per cent of the high energy scattered photons, but it greatly reduced the counting rate in the first counter and, incidentally, the loss due to random anticoincidence of real events. However even with this improvement an anti-coincidence could not be made to work reliably.

The technique adopted was to form coincidences between counters (2) and (3) (the real channel) and from these subtract coincidences between (1), (2) and (3) (the veto channel). As shown in Figure (22), this was done using the negative pulses from the phototubes.

To fulfil the requirement that only events in which an electron-positron pair pass through counters (2) and (3) be considered, the positive pulses from the last dynode of these counters were fed into a pulse height discriminating coincidence

circuit, biased to respond only to two electron pulses.

The output from the discriminating coincidence circuit was put in coincidence with the negative pulses from the tubes: however these had to be delayed 50 musecs. to give the discriminating circuit time to respond.

The outputs of the two coincidence channels (real and veto) were converted to pulses of standard length and height; negative for the real channel and, positive for the veto channel.

Recapitulating at this point, if a high energy photon passes through the telescope converting in the converter a negative pulse occurs in the real channel; if however a charged particle enters the system and starts a shower in the converter then the negative pulse in the real channel is accompanied by a positive pulse in the veto channel.

The subtraction of the "veto" events from the "real" occurs in the slow coincidence anticoincidence circuit. This circuit also performed two other tasks. By demanding the presence of the pulse from the beam gate generator it assured that the event occurred during the millisecond which includes the X-ray beam thus reducing to manageable proportions the background due to cosmic ray showers. One other pulse was necessary before the gate allowing the kicksorter to count was generated. This was a pulse from the discriminator which in turn was triggered by a

pulse over a certain height from the last dynode of the phototube of the Cerenkov spectrometer. Thus, when all these things happened, that is when a photon of over a certain energy (determined by the dynode pulse discriminator) converted in the telescope during the synchrotron beam, the kicksorter was allowed to register the clipped and amplified pulse from the anode of the Cerenkov spectrometer. The system therefore fulfilled all the requirements of the photon scattering experiment.

This was the final system. Initially the pulses from the Cerenkov counter were displayed on an oscilloscope and photographed. This involved the tedious processing and scanning associated with this technique. However the work was not in vain, since the oscilloscope traces obtained showed exactly what was going on in the Cerenkov spectrometer during the beam and gave the author confidence that a kicksorter could be used in the experiment without missing counts or distorting the spectrum of scattered photons.

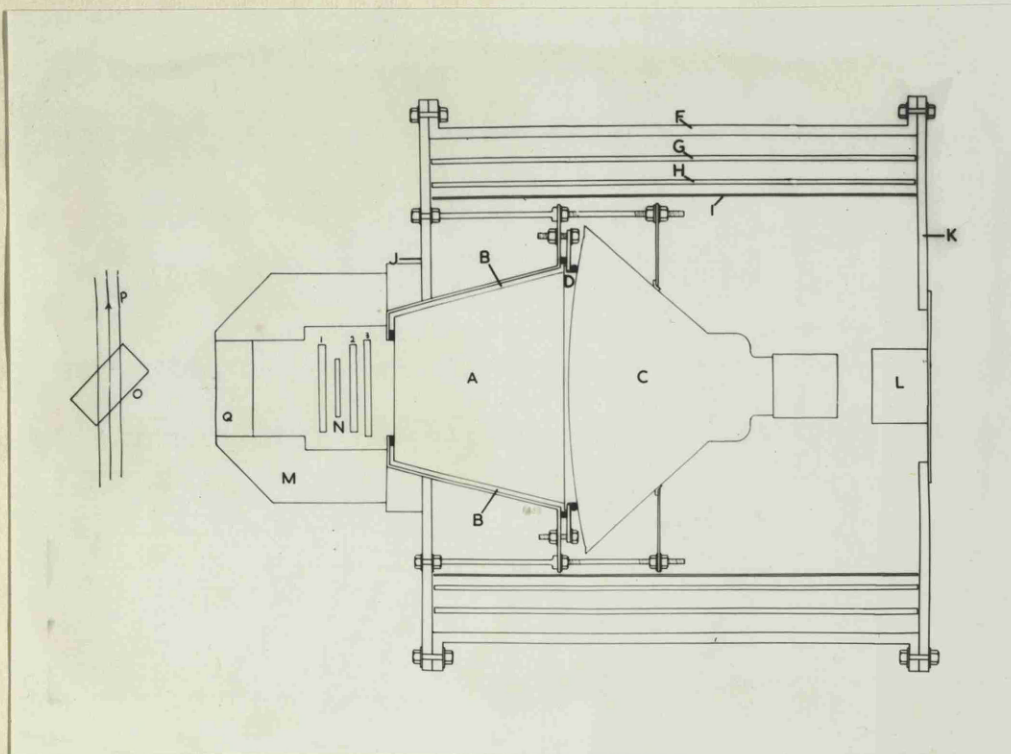
CHAPTER 111.THE PHOTON SCATTERING EXPERIMENT.SECTION 1.General Considerations.

The experiment was performed during two runs on the Glasgow Electron Synchrotron. From the first run of twenty-eight days the relative cross-sections as a function of energy were obtained at 90°, 112° and 135°. During the second run of seven days the absolute cross-section at 90° was measured.

The machine peak energy was reduced to 132 Mev. to prevent the photoproduction of neutral pions whose decay gammas would be indistinguishable from scattered photons. This energy was monitored using the voltage on the condenser bank and also a steady voltage proportional to the maximum current through the magnet coils.

The output of the machine which seldom exceeds 10⁸ equivalent quanta per minute at this energy was monitored by a thick Cornell ionisation chamber (58) coupled to a conventional D.C. amplifier and integrator.

The carbon target used was in the form of a rectangular block of graphite 6 gm/sq.cm. thick (0.13 radiation lengths) placed at 45° to the bremsstrahlen and intercepting the whole beam.



- | | |
|----------|------------------------|
| A - L | See Figure (11) |
| M | Lead Screening |
| N | Lead Converter |
| O | Graphite Target |
| P | X-ray Beam |
| Q | Graphite Filter |
| 1, 2 & 3 | Scintillation Counters |

Figure 23

The Layout of the counter telescope and the Cerenkov Spectrometer for the Photon Scattering Experiment.

The detection system has already been described in detail and the experimental layout is shown in Figure (23). The whole system was mounted on a pivot directly below the target and was therefore easily rotated when required.

The solid angle subtended by the detector was almost $1/10$ of a steradian and under these conditions the rate of accumulation of data was of the order of twenty events per hour.

SECTION 11.

Experimental Procedure.

The apparatus was switched on one-and-a-half hours before the beam became available each day. The first hour allowed the system to stabilise and after this a large series of routine checks were carried out.

The E.H.T. voltage on each phototube was adjusted to the prearranged value using a Cambridge Instrument Company, Vernier Potentiometer with a Weston standard cell as ultimate reference. This enabled the voltage on the counters to be kept constant from day to day to better ^{than} 0.1 per cent.

The stability of the Cerenkov spectrometer was checked by applying the tests described on page 43.

The counters of the telescope were checked with
22 Na and Co⁶⁰ radioactive sources.

The individual counters having been found to be in order, the associated coincidence circuits were tested. The Garwin (52) coincidence circuits used in the experiment have the advantage that any combination of coincidences can be demanded by simple switching. Referring back to Figure (19), both coincidence channels were switched to operate on the pulses from one counter only either (2) or (3). In this mode of operation there should be a one to one correspondance between the

pulses from the real and veto channels. This was then repeated for counters (2) and (3) together.

The formation of the discriminated coincidence of the dynode pulses was checked by turning down the bias to the single particle level and checking that the rate (2) and (3) discriminated was equal to (2) and (3) undiscriminated.

The only part of the electronics remaining to be tested is the slow coincidence-anticoincidence circuit. This was checked by withdrawing one of the required pulses and checking that there was zero output. It was also checked that there was zero output when the output of the real and veto circuits was identical. The discriminator of the Cerenkov spectrometer was checked automatically by observing the low energy cut-off introduced into the cosmic ray spectrum displayed on the kicksorter.

Once started the experiment "ran itself". All that had to be done was to read the kicksorter and the beam integrator and note the duration of each run. The routine tests were carried out about three times per day.

The determination of background was done very simply indeed. The converter was removed from the telescope and the experiment run exactly as before. By calling all counts obtained in this way, "background" and subtracting them, the difference must be events due to the presence of the converter.

The source of this background is partly cosmic ray showers and partly high energy photons and electrons hitting the lead screening of the detector. This second source of background raises the question of whether or not it is a good thing to have any screening at all. However after tests the flux of low energy electrons and photons was regarded as intolerable. It is worth noting that neutrons do not contribute to the background. A neutron entering the counter telescope and giving rise to a knock-on proton in counter (2) would trigger the telescope. However no pulse would come from the Cerenkov spectrometer since unlike a scintillation spectrometer it is totally insensitive to nonrelativistic particles.

The runs described so far are common to nearly all scattering experiments. The type of run to be described now is probably unique to photon scattering experiments. After the ordinary runs and background runs at each angle had been completed, the counter was swung into the incident beam. To enable the electronics to operate satisfactorily the intensity was reduced by a factor of about 5×10^6 . This run was continued for about one day to obtain good statistics. This spectrum plays a very important part in the analysis.

The data obtained so far apart for one important correction are sufficient to give the relative cross-sections as

will be shown in the next chapter. The correction necessary is to compensate for the loss of real events due to random anti-coincidence caused by the high counting rate in the anticoincidence counter. The correction factor was obtained by comparing the following coincidence rates, (2) and (3) alone, (2), (3) and (1) and (2), (3) and (1) in random (i.e. (1) delayed sufficiently to represent a random sample of the beam). This factor was found to be 10 per cent at 90° , 2.5 per cent at 112° and 0.75 per cent at 135° .

Since no counts were obtained when the target was removed, no correction was necessary. Neither were any counts obtained due to random coincidence, again doing away with any need for correction.

SECTION 111.

The Absolute Cross-Section.

The determination of the absolute cross-section involves knowing the efficiency of the detection system. This is not at all simple and the semi-empirical determination of this function is discussed at length in the next chapter.

In the first series of runs using the $\frac{1}{4}$ " lead converter it was found to be virtually impossible to calculate the efficiency with reliable accuracy and the experimental method devised by the author had not yet been conceived. In the second case the $\frac{1}{8}$ " converter enabled an accurate calculation to be carried out.

The problem was to find out how many counts appeared in a particular channel of the kicksorter due to a known number of equivalent quanta incident. The difficulty was the monitoring of the low intensity beam used when the spectrometer was measuring the incident spectrum. The technique which got nearest to success was the following which used the pair spectrometer associated with the synchrotron. The magnet current was adjusted to correspond to pairs of total energy about three quarters of peak energy (100 Mev.) and with a normal beam the Cornell monitor was used to determine the number electron-positron pairs per equivalent quantum. The beam intensity was then reduced by a factor of

over 100 and the pair rate was compared with the rate of single electrons passing down one side of the pair spectrometer.

The Cerenkov spectrometer was then swung into the beam but the time required to obtain reasonable statistics on the number of single electrons when the beam intensity was reduced to the intensity demanded by the electronics associated with the detection system, would have been much too long. This is a reflection of the fundamental problem that a photon measured is a photon lost and therefore the monitoring system if it is not appreciably to affect the beam (which is already exceedingly low in intensity) has an intrinsically low counting rate.

The method devised by the author is exceedingly simple and does not depend on a beam monitor. The efficiency of the detector system was determined by comparing it to the Cerenkov spectrometer itself, which is known to be 100 per cent efficient. The counting rate of the whole system was compared with the counting rate of discriminated dynode pulses from the spectrometer. This gave the mean efficiency between the energy corresponding to the discriminator bias and the peak energy of the machine. Theoretically the efficiency in each energy interval could be obtained by raising the discriminator bias in steps and subtracting. However the errors on the differences proved too large and the time required to obtain accurate values

could not be afforded from the strictly rationed beam time.

The value of approximately twenty per cent average efficiency agreed very well with the theoretical value obtained in the next chapter.

There is one other method of estimating the behaviour of the detection system experimentally. This is to pass mono-energetic electrons through the telescope into the spectrometer. By varying the electron energy and the converter thickness a series of spectra are obtained. The use of these curves simplifies the determination of the efficiency. This was done at M.I.T. but the simplification introduced was not regarded by this group as worth the necessary beam time.

CHAPTER IV.ANALYSIS AND RESULTS.

The calibration, scattering, background and incident bremsstrahlen runs gave the following data:

- 1) A set of resolution curves for different energies.
For the sake of analysis best Gaussian curves were fitted to these and graphs of mean pulse height and standard deviation against energy were thereby obtained.
- 2) The pulse height spectra due to scattering and background and by simple proportionate subtraction, the true spectrum of scattered radiation as seen by the Cerenkov spectrometer and telescope.
- 3) The incident radiation as seen by the Cerenkov spectrometer and telescope.

After allowing for the random anticoincidence loss rate (ibid. p. 58) the relative cross-sections were obtained by dividing the observed scattered spectrum by the observed incident spectrum and using the graph of pulse height against energy. This procedure is justifiable only if the cross-section does not vary too rapidly with energy. For example, if in some hypothetical reaction the cross-section dropped sharply to zero at a certain energy the cross-section, determined by this method, would be

finite in a region beyond the limit, the size of this region being determined by the resolution of the instrument. In the photon scattering, however, no sharp changes of cross-section are expected and hence this technique is valid.

To obtain the absolute cross-sections is a more formidable task. First the behaviour of the detector system must be considered in some detail.

Let us consider what happens to a spectrum of photons incident on the detection system. In passing through the graphite filter some photons will convert into electron-positron pairs and be lost due to the operation of the anticoincidence counter. Since the pair production cross-section is a function of energy the shape of the photon spectrum as well as the total number will be altered. On hitting the lead converter a certain fraction of the photons will convert into pairs and these will begin to lose energy by ionisation. The amount of energy lost by an individual pair will depend on the depth in the converter at which it was formed. A considerable fraction of these photons will share their energy so a symmetrically between the electron and positron that one of these particles will not have enough energy to escape from the converter and pass through counters (2) and (3) and the corresponding photon will therefore be lost.

This critical energy will, of course depend on the

depth of formation of the pair in the converter. The number of photons lost due to this effect increases rapidly as the photon energy is reduced, since the critical energy (for a given depth) becomes a larger fraction of the incident photon energy and therefore a larger area from both ends of the electron-positron energy sharing curve (53) is lost. The effect is further aggravated by the change in the shape of the curve.

From what has been said above it is clear that every point on the original photon spectrum will give rise to a spectrum of pairs and the number of pairs in this spectrum will depend not only on the number of photons but also on their energy.

On entering the Cerenkov spectrometer each point on the pair spectrum gives a Gaussian response of a given mean pulse height and standard deviation.

Thus by folding in all these factors one can predict the response of the system to any given photon spectrum.

It is important, however, to discuss deviations from the simple pattern described above. It is necessary to consider processes which might prevent a member of a pair from passing through the coincidence counters.

The most important factor is multiple scattering of the electrons or positrons. This is one of the main limitations on the thickness of the converter. Indeed it was this effect

that caused the difficulty in the determination of the absolute cross-section in the first series of runs. With the $\frac{1}{8}$ " converter this effect is much less and with the present geometry it can be neglected. The main factor is that the converter is considerably smaller than the counters (2) and (3) and hence electrons or positrons scattered near the edges (55) are not lost. As already mentioned (^{See} *ibid.* p. 31) the M.I.T. telescope did not fulfil this important requirement.

Another process then could cause the loss of a photon is large angle pair production but in the energy region considered the angular distribution is peaked very strongly forward and this effect too can be neglected.

The final process considered is one in which no pair is formed in the first place. This is Compton scattering of the incident photon in the lead converter. However, since pair production overtakes Compton scattering at 5 Mev. in lead this process is also negligible in the energy region considered.

One point worth mentioning is that a member of a pair suffering bremsstrahlung in the converter (in the $\frac{1}{4}$ " twenty per cent did) does not represent an energy loss as it is merely an early start to the shower which will inevitably be produced in the lead glass. If the electron or positron is deflected through a sufficiently large angle then the photon will not

register. This large angle bremsstrahlung (55) was estimated and found to be negligible.

Another point worth noting is the fact that it is impossible to exclude all events due to single electrons in the second and third counters; this is due to the Landau Effect (56) (the asymmetry in the energy loss curve) which enables a single electron to lose an amount of energy usually attributed to two. In general this electron will have been cancelled by the anti-coincidence and even if it came from the lead screening it would have to give this large energy loss in both coincidence counters and hence this effect too is negligible.

Bearing the above considerations in mind, the author can now describe how he calculated the response of the detector system to the bremsstrahlung spectrum and hence evaluated the absolute cross-sections.

The processes involved were too complicated to treat analytically and hence the whole calculation was carried out numerically.

First the Schiff (57) thin target bremsstrahlung spectrum was calculated for an electron energy of 132 Mev. This spectrum was normalised to 1000 equivalent quanta and then, for the purpose of the calculation converted to a histogram of class width 5 Mev., all photons in each strip being regarded as

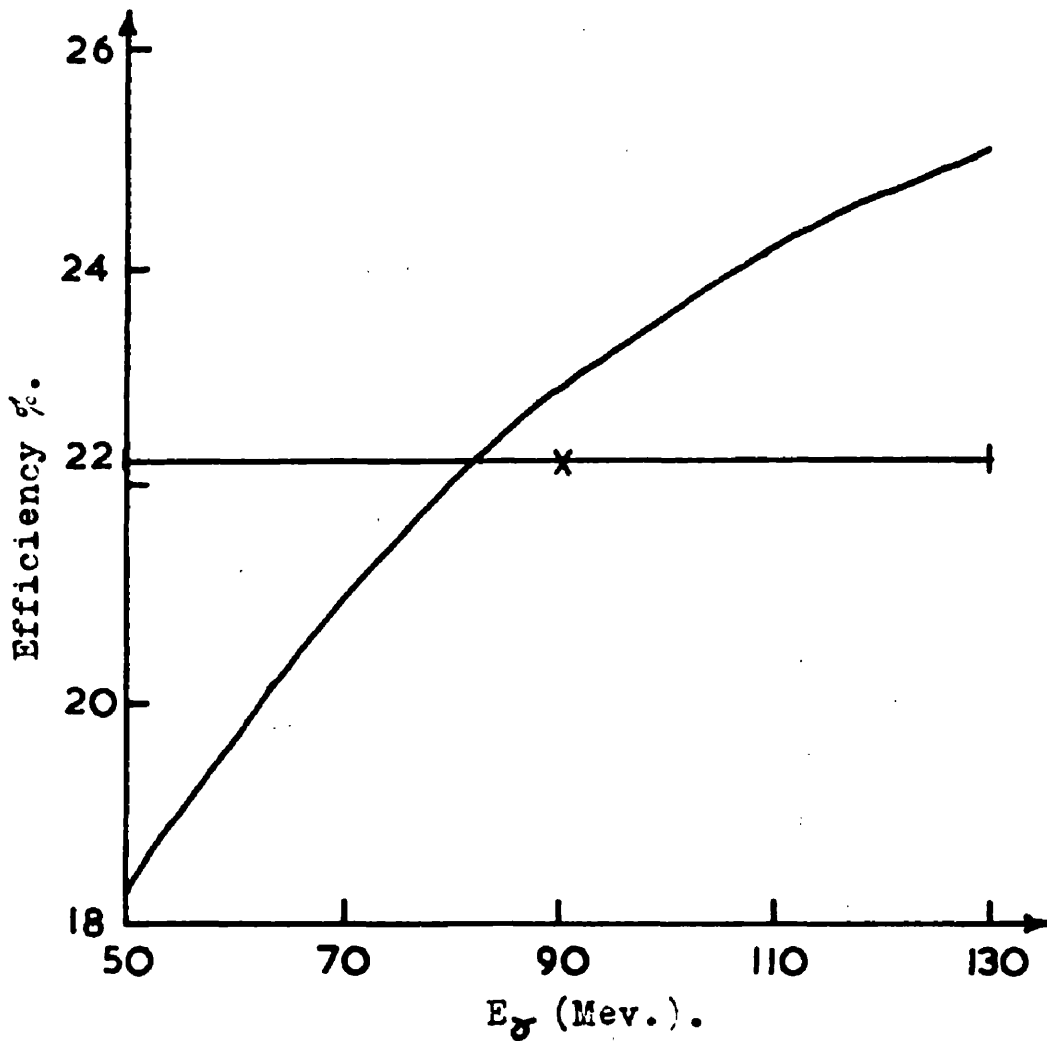
having the energy of the class mark.

The attenuation of the beam due to pair production in the graphite filter was calculated and the number of photons in each class was altered accordingly, the classes themselves remaining, of course, unaltered.

For the purpose of calculation the converter was regarded as being made up of strips; four in the case of the $\frac{1}{4}$ " and two in the case of the $\frac{1}{8}$ ". Using more would have been a waste of time since the classes used for the bremsstrahlung spectrum were already 5 Mev. wide. The number of pairs formed in each section was calculated and each pair was regarded as coming from the middle (not strictly true) of the strip in which it was formed.

The minimum energy of electron which could pass through the rest of the telescope was calculated for each section. The fraction of photons which give rise to electrons or positrons of less than this energy was calculated by counting the squares under the energy sharing curves (53) corresponding to that photon energy.

This alters the number of photons in each energy class but does not distort the classes themselves. The change in the classes is due to the ionisation energy loss of the pair formed by the incident photon in traversing the rest of the



E_γ (Mev.).

Fig. 27.

Semi-empirically Predicted Efficiency and the
Experimental Mean Value.

Pulses per Channel Due to 1000 Equivalent
Quanta of 132 Mev. Peak Bremsstrahlen.

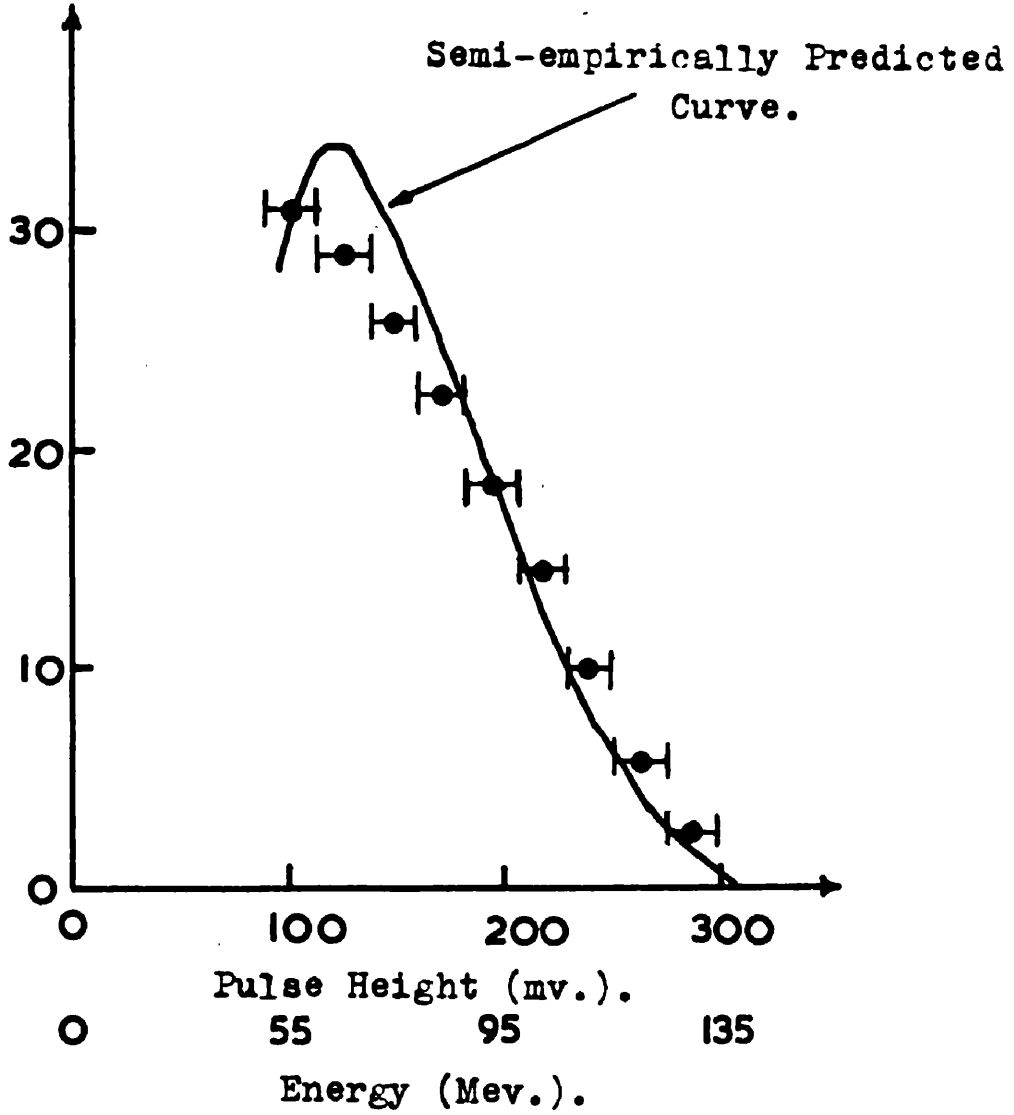


Fig. 24.

The Response of the Detection System to the
Bremsstrahlen.

converter and the coincidence counters.

Thus each photon group gives rise to two or four groups of pairs with a different number in each.

These groups were redistributed into a new histogram giving the number of pairs in each 5 Mev. interval incident on the Cerenkov spectrometer. Each class in this new histogram was converted into a Gaussian curve of mean pulse height and standard deviation determined from the calibration runs.

The contribution of each Gaussian to each pulse height interval was calculated using standard tables of the area under error curves. Addition of these contribution gave the semi-empirically predicted response to the bremsstrahlen. Figure (24) shows the predicted curve and the experimental points from the bremsstrahlen run described on page 57 ; the experimental points are normalised to the same number of pulses and pulse height interval..

It is important to stress that the numbers on the vertical scale of this graph really mean something. They give the number of pulses obtained in a given pulse height interval due to 1000 equivalent quanta of 132 Mev. bremsstrahlen. Thus, knowing the relative scattering cross-sections and the total number of equivalent quanta used in each run, the absolute cross-section can be obtained. These cross-sections are shown in

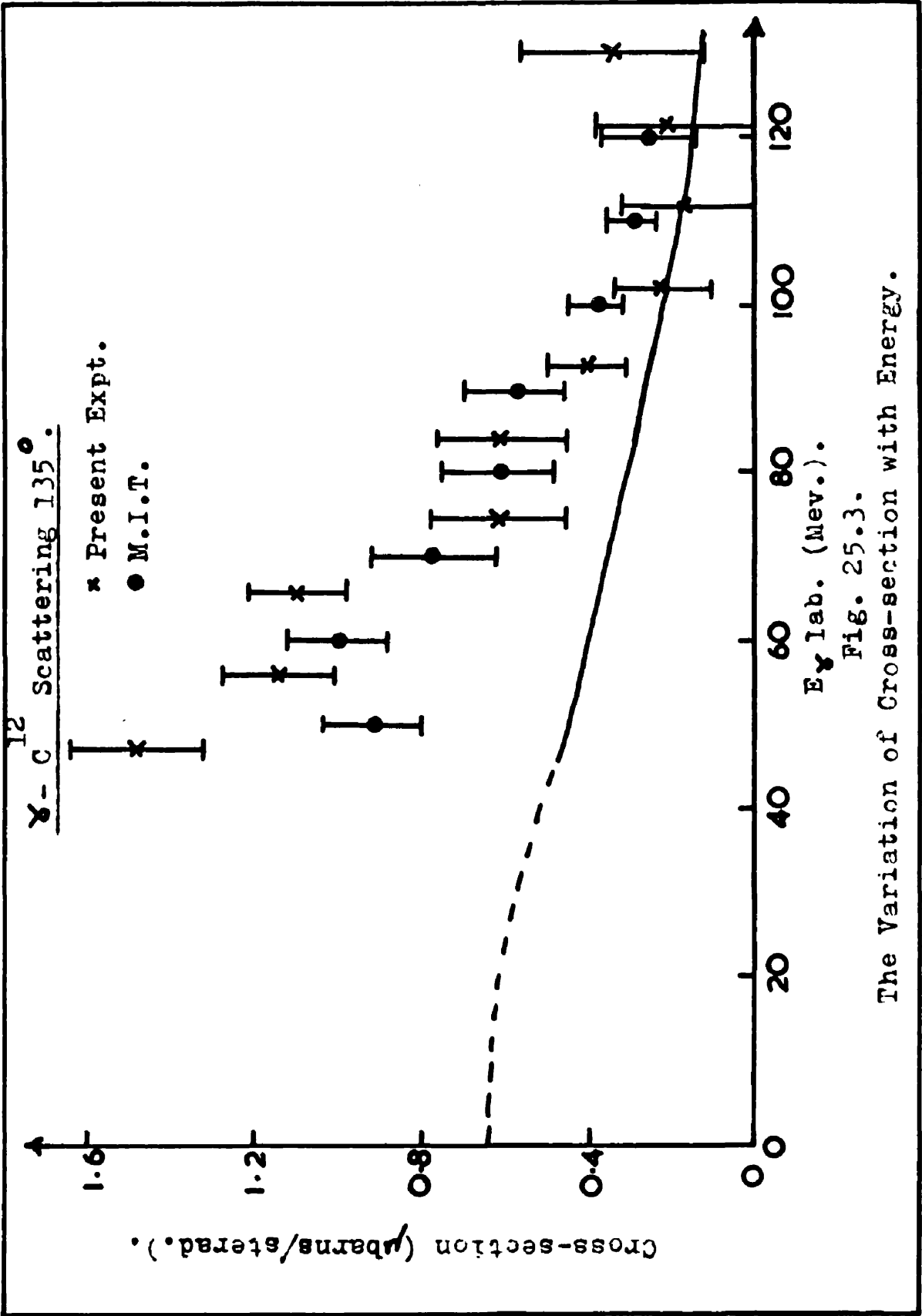
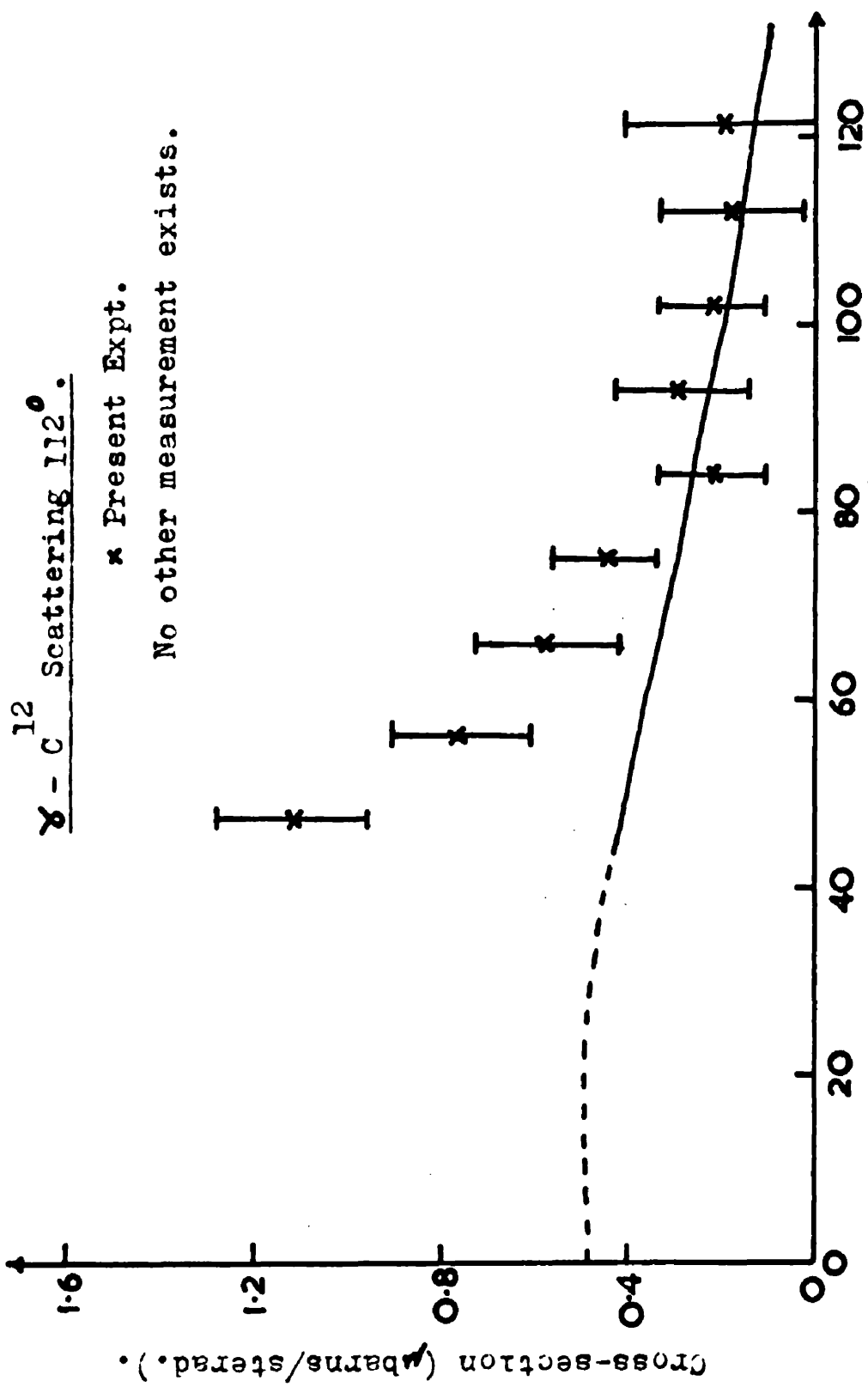


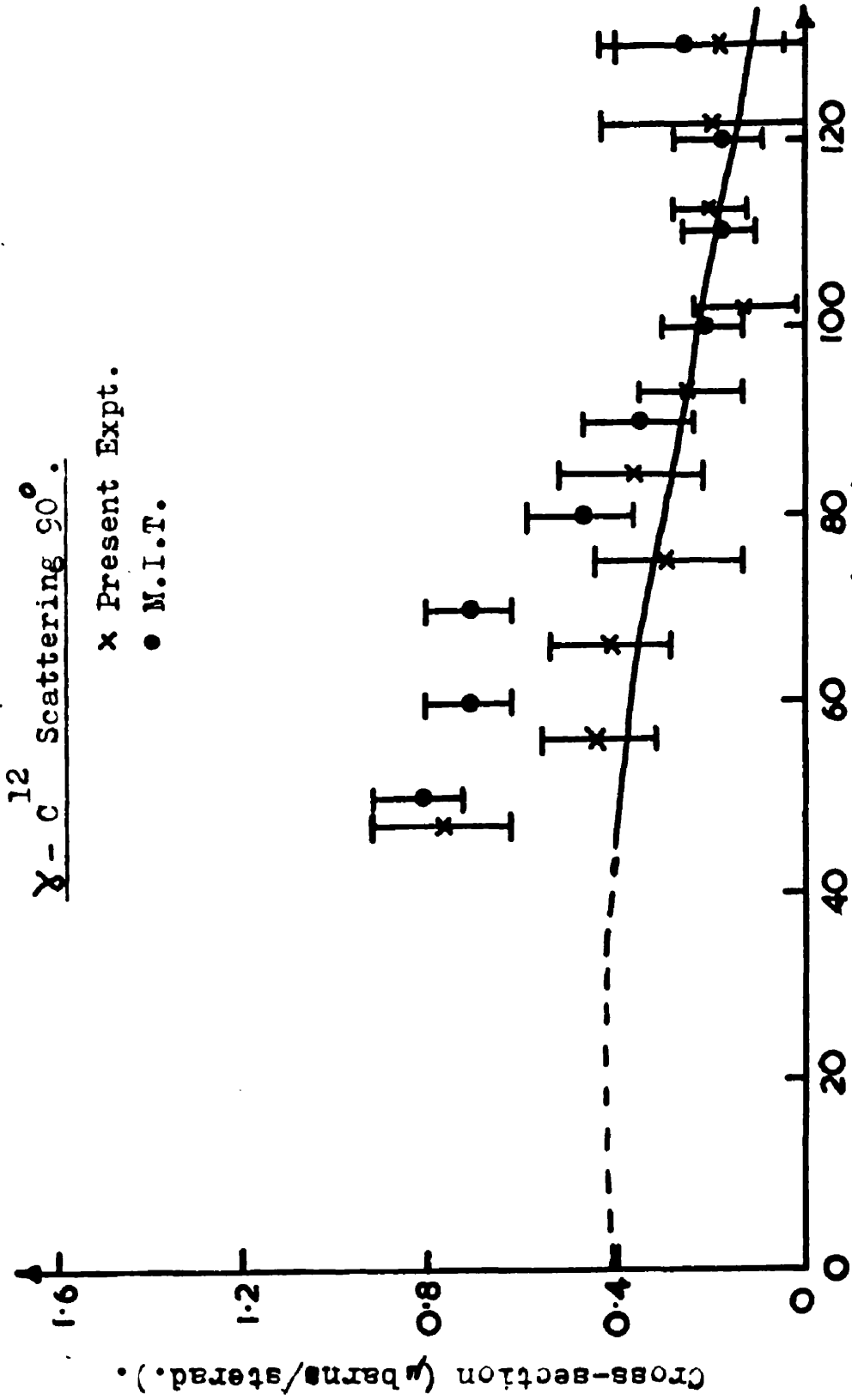
Fig. 25.3.

The Variation of Cross-section with Energy.



E_{lab.} (Mev.).
Fig. 25.2.

The Variation of Cross-section with Energy.



E_γ Lab. (Mev.).

Fig. 25.1.

The Variation of Cross-section with Energy.

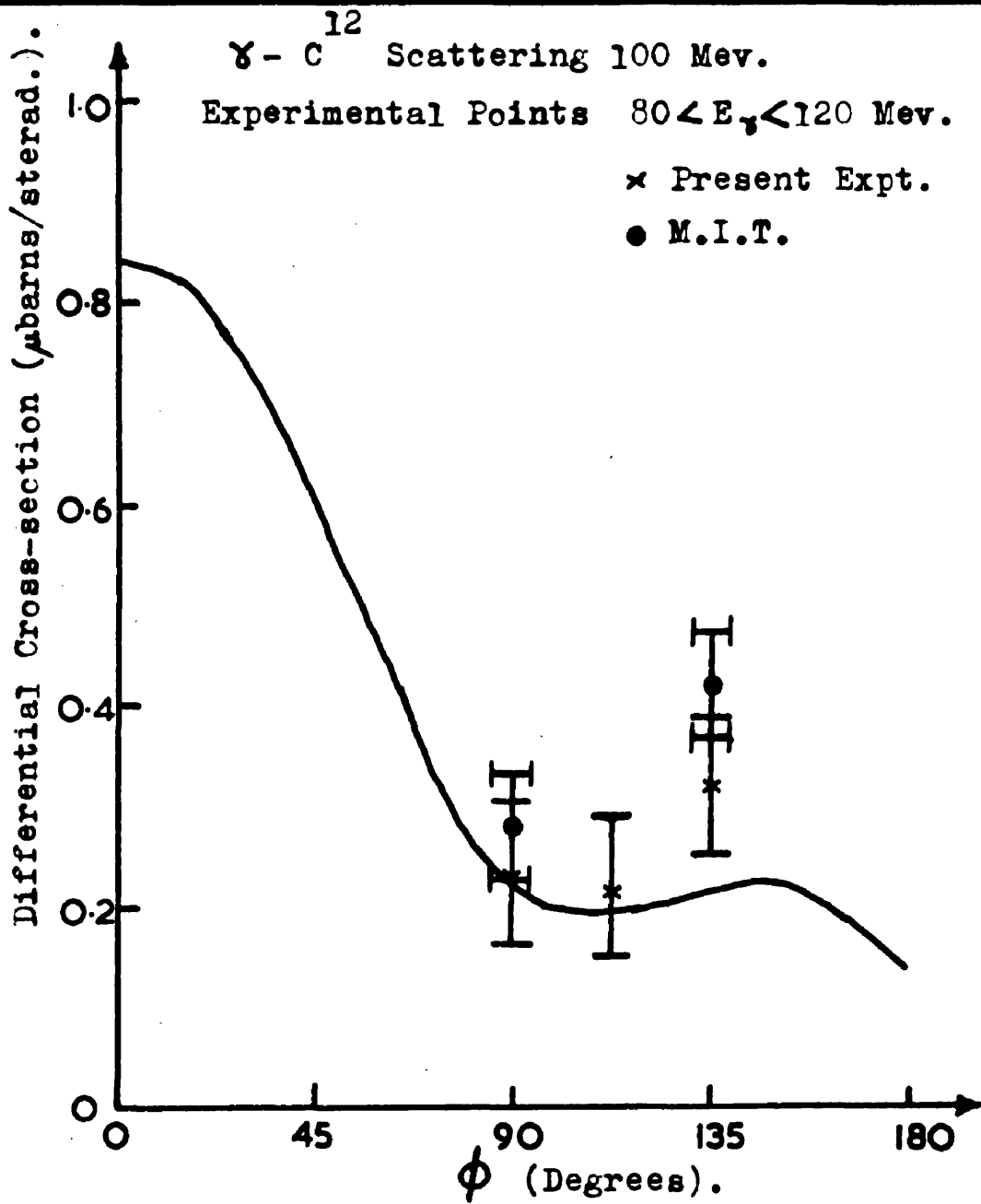


Fig. 26.

Experimental Angular Distribution.

Note. There is a $\pm 10\%$ uncertainty in the absolute values of both the Glasgow and M.I.T. results given in figures 25 and 26.

Figures (25) and (26) together with the results of the M.I.T. group and the theoretical predictions. The discussion of these results is contained in the next chapter and therefore no further comment is made here.

From what has already been said it will have been realised that it is difficult to define the efficiency of the detection system, as a photon, if detected, can appear in almost any energy channel. What was measured experimentally (p. 60) was the probability that the photons from a certain energy upwards were detected at all.

This mean value is compared with the calculated value which has been shown as a function of energy on Figure (27).

The maximum error introduced into the absolute cross-section by the approximations and uncertainties in the calculation is $\sim \pm 10$ per cent. This is true of both the Glasgow and M.I.T. results.

CHAPTER V.DISCUSSION AND CONCLUSIONS.

On first looking at Figure (25) one despairs of reconciling the experimental points and the theoretical curves. The points are definitely too high at the low energy end and tend to be the same at the high energy end. The fit in the centre region is not too bad. Thus one may say that the assumptions made in the derivation of the theoretical curve are not valid in the low energy region and are also becoming doubtful near the end of the high energy region.

The low energy region is reconciled by saying that the excess is due to the tail end of the nuclear resonance scattering. This is equivalent to saying that postulate one (page 12), that the nucleons are free in intermediate states, is not true.

The rising trend near meson threshold is more pronounced at 135° than any other angle; this supports the attribution of the excess to effects associated with nucleon structure, since it has been shown (^{See} ~~ibid.~~ p. 9) that the magnetic dipole amplitude associated with interaction with the meson field is in phase with the electric dipole Thomson amplitude in the backward direction.

Thus in the region from 80 Mev. to nearly meson threshold the simple theory seems to fit fairly well. Hence the assumptions made in the introduction appear to be valid. Therefore the conclusions to be drawn from the experiment are: The nucleons can be regarded as free in intermediate states in this region or returning to the language of the first page of this thesis; the carbon nucleus when viewed by electro-magnetic radiation of de Broglie wavelength comparable to its own dimensions seems to be composed of individual nucleons not associated with each other in subgroups.

The second assumption that the impulse approximation is valid is largely a reiteration of assumption (1), it does however, suggest that no multiple scattering is occurring or, simply, the radiation scattered by one nucleon is not rescattered by another before it leaves the nucleus. This is equivalent to saying that the nucleus is almost transparent to light of this wavelength.

The third assumption has already been mentioned in this section. It seems that in this case the mesonic polarisability has affected the cross-section sooner than expected but, in the narrow region between 80 and 110 Mev., the effect due to the anomalous magnetic moment is indeed quenched in the carbon nucleus, probably due to the cancelling of the spins as suggested.

REFERENCES

1. W. Thirring,
Phil. Mag. 41, 1193 (1950).
2. F. E. Low,
Phys. Rev. 96, 1428 (1954).
3. M. Gell-Mann and M. L. Goldberger,
Phys. Rev. 96, 1433 (1954).
4. W. Pauli,
Rev. Mod. Phys. 13, 203 (1941).
5. J. L. Powell,
Phys. Rev. 75, 32 (1949).
6. R. G. Sachs and L. L. Foldy,
Phys. Rev. 80, 824 (1950).
7. R. H. Capps and W. G. Holladay,
Phys. Rev. 99, 931 (1955).
8. W. J. Karzas, W. K. R. Watson and F. Zachariasen,
Phys. Rev. 110, 253 (1958).
9. N. Austern,
Phys. Rev. 100, 1522 (1955).
10. S. Minami,
Progr. Theoret. Phys. 9, 108 (1953).
11. V. I. Ritus,
J. Exp. Theor. Phys. (USSR) 30, 1070 (1956).
Translation. Soviet Phys. 3, 926 (1957).
12. R. I. Gurzhi,
J. Exp. Theor. Phys. (USSR) 30, 1079 (1956).
Translation. Soviet Phys. 3, 941 (1957).
13. B. T. Feld,
Annals of Physics 4, 189 (1958).
14. G. Bernardini,
Proc. 7th. Annual Rochester Conference I-31.

(contd)

REFERENCES

15. L. G. Hyman, R. Ely, D. H. Frisch and M. A. Wahlig,
Phys. Rev. Letters 3, 93 (1959).
16. M. Gell-Mann, M. L. Goldberger and W. E. Thirring,
Phys. Rev. 95, 1612 (1954).
17. R. H. Capps,
Phys. Rev. 106, 1031 (1957).
18. M. Cini and R. Stroffolini,
Nuclear Physics 5, 684 (1958).
19. G. F. Chew,
Proceedings of the 1958 CERN Conference on
High Energy Physics page 98.
20. J. M. Blatt and V. F. Weisskopf,
"Theoretical Nuclear Physics" Chapman and Hall Limited,
London, 3rd. ed. 1956, page 319.
21. Z. Maric and P. Mobius,
Nuclear Physics 10, 135 (1959).
22. R. Gomez,
Ph.D. thesis, Massachusetts Institute of Technology,
1956. (unpublished).
23. G. E. Pugh, R. Gomez, D. H. Frisch and G. S. Janes,
Phys. Rev. 105, 982 (1957).
24. A. H. Compton and S. K. Allison,
"X-rays in Theory and Experiment" 2nd. ed.
D. Van Nostrand Co. Inc. New York (1949) page 137.
25. G. E. Brown and J. B. Woodward,
Proc. Royal Soc. (London) A65, 977 (1952).
26. L. W. Alvarez, F. S. Crawford Jr. and M. L. Stevenson,
Phys. Rev. 112, 1267 (1958).
27. C. L. Oxley and V. L. Telegdi,
Phys. Rev. 100, 435L (1955).

(contd)

REFERENCES

28. C. L. Oxley,
Phys. Rev. 110, 733 (1958).
29. Govorkov, Goldanski, Kárpukhin, Katsenko and Pavlovskaya,
Doklady Akad. Nauk. SSSR 111, 988 (1956).
Translation. Soviet Physics Doklady 1, 735 (1956).
30. G. Bernardini,
Proc. CERN Symposium, 1956, page 261.
31. R. M. Littauer, J. W. DeWire and M. Feldman,
Bull. Am. Phys. Soc. 4, 253 (1959).
32. H. R. Kratz, J. Rouvina and W. B. Jones,
Bull. Am. Phys. Soc. 4, 253 (1959).
33. J. L. Burkhart,
Phys. Rev. 100, 192 (1955).
34. W. Franz,
Z. Physik 98, 314 (1936).
35. J. S. Levinger,
Phys. Rev. 87, 656 (1952).
36. F. Rohrlich and R. L. Gluckstern,
Phys. Rev. 86, 1 (1952).
37. H. A. Bethe and F. Rohrlich,
Phys. Rev. 86, 10 (1952).
38. H. A. Bethe private communication to R. R. Wilson,
Phys. Rev. 90, 720 (1953).
39. P. B. Moon,
Proc. Phys. Soc. (London), A64, 76 (1951).
40. P. B. Moon and Storruste,
Proc. Phys. Soc. (London) A66, 585 (1953).
41. K. G. Malmfors,
Ark. Fys. 6, 49 (1953).
42. E. G. Fuller and E. Hayward,
Phys. Rev. 101, 692 (1956).

(contd)

REFERENCES.

43. M. B. Stearns,
Phys. Rev. 87, 706 (1952).
44. G. E. Pugh, D. H. Frisch and R. Gomez,
Phys. Rev. 95, 590L (1954).
45. R. Gomez, G. E. Pugh, D. H. Frisch and G. S. Janes,
Phys. Rev. 100, 1245A (1955).
46. A. Kantz and R. Hofstadter,
Nucleonics, 12, 36 (1954).
47. P. A. Cerenkov,
Phys. Rev. 52, 378 (1937).
48. J. M. Cassels, G. Fidecaro, A. M. Wetherwell and
J. R. Wormald,
Proc. Phys. Soc. 70A, 405 (1957).
49. W. B. Jones, H. R. Krantz and J. Rouvina,
Rev. Sci. Inst. 28, 167 (1957).
50. J. Moffatt and M. W. Stringfellow,
Jour. Sci. Inst. 35, 18 (1958).
51. W. S. C. Williams and H. S. Caplan,
Nature Vol. 179, 1185 (1957).
52. R. L. Garwin,
Rev. Sci. Inst. 21, 569 (1952).
53. W. Heitler,
"The Quantum Theory of Radiation",
Oxford Univ. Press, 3rd. ed. page 261.
54. J. Crear, A. H. Rosenfeld and R. A. Schluter,
"Nuclear Physics" A course given by E. Fermi.
The Univ. of Chicago Press. Revised Edition, page 36.
55. R. C. Miller,
Phys. Rev. 95, 796 (1954).

(contd)

REFERENCES

56. L. Landau,
J. Phys. (U.S.S.R.) 8, 201 (1944).
57. L. I. Schiff,
Phys. Rev. 83, 252 (1951).
58. R. R. Wilson,
Nuclear Instruments 1, 101 (1957).